

Montmorillonite stability

With special respect to KBS-3 conditions

Ola Karnland, Martin Birgersson
Clay Technology AB

August 2006

Svensk Kärnbränslehantering AB

Swedish Nuclear Fuel

and Waste Management Co

Box 5864

SE-102 40 Stockholm Sweden

Tel 08-459 84 00

+46 8 459 84 00

Fax 08-661 57 19

+46 8 661 57 19



Montmorillonite stability

With special respect to KBS-3 conditions

Ola Karnland, Martin Birgersson
Clay Technology AB

August 2006

This report concerns a study which was conducted for SKB. The conclusions and viewpoints presented in the report are those of the authors and do not necessarily coincide with those of the client.

A pdf version of this document can be downloaded from www.skb.se

Abstract

The basic advantageous properties, e.g. low hydraulic conductivity and high swelling pressure, of the bentonite buffer in a KBS-3 repository stem from a strong interaction between water and the montmorillonite mineral in the bentonite.

Minerals similar in structure but with substantially lower mineral-water interaction exist in nature. Transformations from montmorillonite to such minerals are observed e.g. in burial diagenesis and in contact metamorphism. A thermodynamic consideration confirms that medium and low charged montmorillonite is not in chemical equilibrium with quartz. From a safety assessment perspective it is therefore of vital importance to quantify the montmorillonite transformation under KBS-3 conditions.

Silica release from the montmorillonite tetrahedral layers is the initial process for several possible transformations. Replacement of silica by aluminum increases the layer charge but maintains the basic atomic structure. A sufficiently high layer charge results in an irreversible collapse of the clay-water structure, i.e. a non-swelling mineral is formed. Compared to other cations, potassium as counter ion leads to a collapse at lower layer charge and the produced phase is generally termed illite.

Montmorillonite-to-illite transformation is the most frequently found alteration process in nature. Three different kinetic illitization models are reviewed and the model proposed by Huang et al. is considered the most suitable for quantification in a KBS-3 repository, since the kinetic rate expression and its associated parameters are systematically determined by laboratory work. The model takes into account temperature, montmorillonite fraction and potassium concentration, but do not include relevant parameters such as pH, temperature gradients and water content. Calculations by use of the Huang illitization model applied for repository conditions yield insignificant montmorillonite transformation also under very pessimistic assumptions.

Other non-swelling minerals, e.g. chlorite and rectorite, may be formed in processes similar to illitization. However, there are no indications, neither from laboratory work nor from natural analogs, that these processes should be faster than illitization.

A relatively fast layer charge increase may be caused by reduction of montmorillonite structural iron. The maximum effect of the reduction on mineral-water interaction depends on the initial layer charge and the total amount of structural iron.

Migration of small cations into the montmorillonite octahedral layer reduces the layer charge at temperatures significantly higher than the maximum temperature in a KBS-3 repository. The extent of the migration at repository temperature remains to be determined.

Processes causing breakdown of the montmorillonite atomic structure takes place under extreme conditions not expected in a KBS-3 repository. Substantial dissolution of montmorillonite is expected above pH 11 since new aqueous silica species start to dominate in this pH range. Recent laboratory studies also indicate that close contact with metallic iron may result in a destabilization of the montmorillonite structure.

Based on the present knowledge, none of the identified transformation processes are expected to lead to significant reduction of the buffer performance. However, uncertainties remain concerning silica diffusivity, kinetics of octahedral layer charge reduction, and interaction between metallic iron and montmorillonite.

Sammanfattning

De grundläggande fördelaktiga buffertegenskaperna, t. ex. låg hydraulisk konduktivitet och högt svälltryck, i ett KBS-3-slutförvar beror på stark växelverkan mellan vatten och mineralet montmorillonit i bentoniten.

Mineral med likartad struktur men med avsevärt mindre växelverkan med vatten förekommer i naturen. Omvandling från montmorillonit till sådana mineral har påvisats bl. a. vid sedimentdiagenes och kontaktmetamorfos. En termodynamisk betraktelse bekräftar att låg- och medelladdad montmorillonit inte är i kemisk jämvikt med kvarts. Ur ett säkerhetsperspektiv är det därför av avgörande betydelse att kvantifiera montmorillonitomvandlingen vid KBS-3-förhållanden.

Kiselaavgång från montmorillonitens tetraederlager är startprocessen för flera tänkbara mineralomvandlingar. Aluminium som ersättning för kisel ökar flakladdningen men bevarar den grundläggande atomstrukturen. Vid tillräckligt hög flakladdning inträffar en irreversibel kollaps av lera-vattenstrukturen, d.v.s. ett icke svällande mineral bildas. Kalium som motjon leder till kollaps vid lägre flakladdning i jämförelse med andra katjoner och den bildade fasen benämns allmänt illit.

Montmorillonit till illit är den mest observerade omvandlingsprocessen i naturen. Tre olika kinetiska illitiseringsmodeller har därför jämförts och modellen framtagen av Huang et al. bedöms som mest lämpad för kvantifiering av illitisering i ett KBS-3-slutförvar eftersom det kinetiska uttrycket och alla associerade parametrar är systematiskt bestämda genom laboratorieförsök. Modellen hanterar temperatur, montmorillonithalt och kaliumkoncentration men saknar hantering av relevanta parametrar som pH, temperaturgradienter och vattenhalt. Beräkningar med Huangs illitiseringsmodell för slutförvarsförhållanden ger obetydlig omvandling av montmorilloniten även under mycket pessimistiska antaganden.

Andra icke-svällande mineral som t. ex. klorit och rektorit kan bildas i processer som liknar illitisering. Det finns emellertid inga laboratorieresultat eller naturliga analogier som tyder på att dessa processer skulle vara snabbare än illitisering.

En relativt snabb flakladdningsökning kan orsakas av reduktion av järn i montmorillonitens atomstruktur. Reduktionens maximala effekt på mineralets växelverkan med vatten beror på mängden strukturellt järn samt på den ursprungliga flakladdningen.

Migration av små katjoner in till montmorillonitens oktaederlager minskar flakladdningen vid temperaturer som är betydligt högre än maximitemperaturen i ett KBS-3 slutförvar. Omfattningen av denna migration vid förvarstemperaturer återstår att fastställa.

Vissa extrema förhållanden, som inte förväntas i ett KBS-3-förvar, leder till nedbrytning av montmorillonitens atomstruktur. Omfattande upplösning av montmorillonit kan förväntas vid pH över 11 eftersom nya vattenlösta kiselspecier börjar dominera i detta pH-område. Nyligen genomförda laboratorieförsök indikerar också att närkontakt med metalliskt järn kan resultera i en destabilisering av montmorillonitstrukturen.

Ingen av de identifierade omvandlingsprocesserna förväntas leda till påtaglig försämring av buffertegenskaperna baserat på nuvarande kunskapsläge. Osäkerheter kvarstår emellertid för diffusion av kisel, för kinetiken i processen som leder till minskad oktaederladdning, och för reaktioner mellan metalliskt järn och montmorillonit.

Innehåll

| | | |
|-------------------|---|----|
| 1 | Background | 7 |
| 1.1 | General | 7 |
| 1.2 | Montmorillonite structure | 7 |
| 1.3 | Sealing properties of montmorillonite | 8 |
| 1.4 | Repository conditions | 9 |
| 2 | Montmorillonite transformation processes | 11 |
| 2.1 | General | 11 |
| 2.2 | Stability considerations | 12 |
| 2.3 | Transformation processes | 13 |
| 2.4 | Illitization | 14 |
| | 2.4.1 Kinetic models of illitization | 17 |
| | 2.4.2 Kinetic model review | 18 |
| 3 | KBS-3 specific discussion | 23 |
| 3.1 | Quantification of possible illitization | 23 |
| | 3.1.1 Potassium availability | 23 |
| | 3.1.2 Illitization modeling results | 24 |
| | 3.1.3 Calculation uncertainties | 24 |
| 3.2 | Other possible alteration processes | 25 |
| | 3.2.1 Chloritization | 25 |
| | 3.2.2 Fixation of other ions than potassium | 26 |
| | 3.2.3 Silica release due to high pH | 26 |
| | 3.2.4 Temperature gradient induced silica release and transport | 28 |
| | 3.2.5 Redox-reaction induced octahedral layer changes | 29 |
| | 3.2.6 Temperature induced octahedral layer charge changes | 30 |
| 3.3 | Effects of montmorillonite alteration | 30 |
| | 3.3.1 General | 30 |
| | 3.3.2 Minor layer charge changes | 31 |
| | 3.3.3 Illitization | 31 |
| | 3.3.4 Chloritization | 32 |
| 4 | Summary and conclusions | 33 |
| | References | 35 |
| Appendix 1 | Summary of the three reviewed illitization models described in section 2.4.1 and 2.4.2. | 39 |

1 Background

1.1 General

Several concepts for HLW repositories involve bentonite for canister embedding because of the suitable physical properties, e.g. low hydraulic conductivity, swelling ability and rheological behavior. These properties are determined by the interaction between water and the smectite component, which usually is montmorillonite. Other minerals with the same principal structure as montmorillonite, but with different layer charge, occur in nature, and transitions and intermediate stages are frequently present. Some of these related minerals have radically different sealing properties than montmorillonite, and the stability of montmorillonite is consequently of vital importance for the performance of the buffer in a KBS-3 repository. The demand on the buffer is that the major part of montmorillonite remains intact during the repository lifetime. Fortunately, the mineralogical stability of montmorillonite has been extensively studied, mainly because the smectite-to-illite transformation may serve as a geo-thermometer for predicting source rock maturation in oil prospecting. The transformation has also received a great deal of academic interest because of both the disputed structure of mixed-layer illite/smectite and of the reaction mechanism. This report aims at giving a general description of the minerals related to possible montmorillonite transformation, transformation reactions, and discusses the present means to quantify such processes.

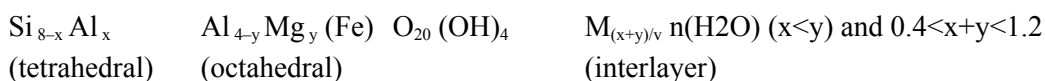
1.2 Montmorillonite structure

High quality commercial bentonites normally contain over 80% of montmorillonite, which gives different bentonite products similar properties in many respects. The distribution of accessory minerals may vary within, and especially between, different quarries. Typical accessory minerals are feldspars, quartz, cristobalite, gypsum, calcite and pyrite.

The montmorillonite mineral belongs to the smectite group, in which all the minerals have an articulated layer structure. The thickness of an individual mineral layer is around 1 nm and the extension in the other two directions is often several hundred nanometers (Figure 1-1). Each layer is composed of a central sheet of octahedrally coordinated cations, which on both sides is linked through shared oxygens to sheets of tetrahedrally coordinated cations. Clay minerals of this type are often referred to as a 2:1 layer structures.

By definition of the montmorillonite mineral, the following applies. The octahedral sheet has aluminum as central ion, which is partly substituted, principally by Mg. The tetrahedral sheet has silicon as central ion, which may partly be substituted, principally by aluminum. The substitutions result in a net negative charge of the montmorillonite layer in the range of 0.4 to 1.2 elementary charges per unit cell ($O_{20}(OH)_4$), and the octahedral charge is larger than the tetrahedral. The induced negative layer charge is balanced by cations (M), with the valence v , located between the individual layers (interlayer space). A variable number (n) of water molecules may be intercalated between the individual mineral layers /Newman 1987/.

The ideal montmorillonite formula may consequently be written:



and the structure may schematically be illustrated as in Figure 1-1.

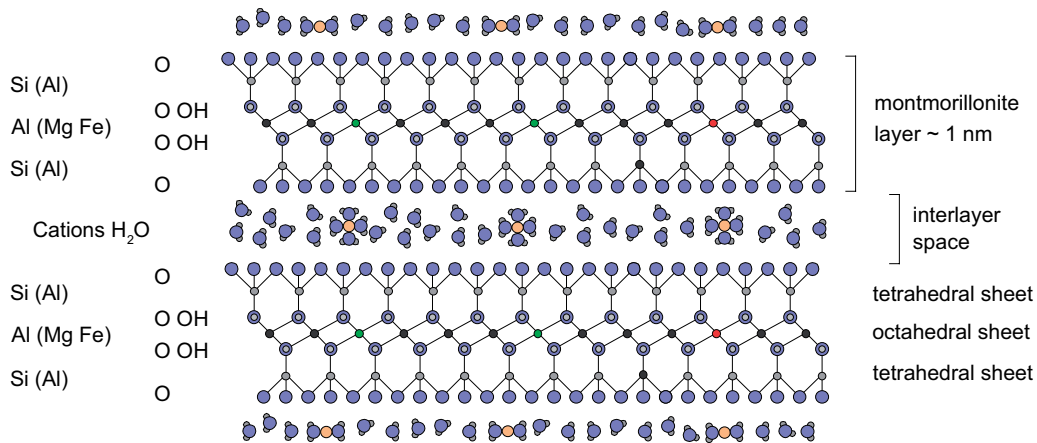


Figure 1-1. Edge view cartoon of two montmorillonite layers with interlayer cations and water molecules.

1.3 Sealing properties of montmorillonite

Generally, ions in a water solution reduce the water chemical potential, and a concentration difference between solutions normally leads to water transport from the high potential (low concentration) to the low potential volume. In parallel, ions diffuse from the high concentration to low concentration volume, and the equilibrium condition, i.e. equal chemical potentials, leads to uniform ion concentration.

In bentonite, the conditions are extraordinary due to the negatively charged montmorillonite layers and the charge compensating cations in the interlayer space. Water molecules can hydrate the cations and create an interlayer ionic solution. But, the cations cannot freely diffuse away from the mineral surface because of the demand for electrical neutrality. Water will consequently be transported into the interlayer space, if water with a higher chemical potential is available, and the interlayer distance will increase, which is synonymous with bentonite swelling. This water uptake will continue until the chemical potentials equalize, which in the case of a pure water source theoretically leads to infinite swelling. The extent of water uptake in bentonite may thereby be orders of magnitude larger and have a different character than in other soil materials.

In a fixed total volume, the water uptake into the interlayer space will reduce the volume of initially larger pores. The uptake is forced to stop when the total available pore volume is completely filled with introduced water. At this full water saturation, water will continue to move internally in order to level the interlayer ion concentration and thereby the chemical potential in the system. The interlayer distances will thus increase in interlayer space with high concentration at the expense of interlayer space with low concentration, and the final distances will be a function of the local montmorillonite layer charge. The remaining difference in ion concentration, between the high concentration interlayer solution and the water supplying solution, leads to an osmotic pressure build-up in the bentonite, generally termed swelling pressure, which equalizes the chemical potential in the system. The homogenization of the pore size, due to the levelling of the chemical potential, may be partly counteracted by mechanically stable structures, e.g. in volumes with complicated stacking of the montmorillonite layers, or in clusters of accessory minerals. In extreme cases the pore-water in such clusters may eventually be in equilibrium with the water supplying solution, without influence from the surrounding montmorillonite charge compensating cations.

The degree of final pore-size homogeneity has been analyzed and extensively discussed in the literature, and quite different conceptual and quantitative models have been proposed. The conditions are of major importance since the pore-size distribution governs both the diffusive

and advective transport capacity of the system. However, the conditions lead to a systematic distribution of water between the montmorillonite layers, which in turn lead to the characteristic swelling properties and very restricted transport capacity.

Increasing the bentonite density leads to less water in the system and shorter distances between the montmorillonite layers. Figure 1-2 shows the measured swelling pressure and hydraulic conductivity in MX-80 bentonite for a wide range of densities and groundwater salinities.

1.4 Repository conditions

In the KBS-3 concept, montmorillonite will be present in the bentonite buffer material and in the tunnel backfill material (Figure 1-3). The montmorillonite content in the buffer will be around 80%, and the final target buffer density after water uptake will be $2,000 \text{ kg/m}^3 \pm 50 \text{ kg/m}^3$ (dry density of $1,570 \text{ kg/m}^3$) which corresponds to a swelling pressure of approximately 7 MPa.

During the initial saturation phase, water will be sucked into the bentonite mainly from fractures and the tunnel backfilling material. The acceptance criteria for a deposition hole will guarantee that the fractures are relatively small and the fracture frequency low. The possible interaction between the buffer bentonite and the surrounding groundwater will consequently be very limited through fractures, and practically none through the intact rock.

The possible interaction with the tunnel backfilling material, i.e. the pore volume contact, will be much larger. On the other hand, the buffer thickness above the canister is 1.5 m compared to 0.35 m between the canister and the rock. The system may consequently be considered as relatively closed. The geochemical conditions in the major part of the buffer will thereby be largely controlled by the choice of bentonite type and the initially saturating groundwater for a relatively long period of time. However, the buffer has to be treated as an open system in the long term perspective, and the extent of the interaction may be of decisive importance for the montmorillonite transformation.

The conditions are similar to those in deep-sea sediments, in which smectite transforms over geological time scales, and we can expect similar processes in a repository. The basic reason for the transformation is thermodynamic non-equilibrium, and in the case of montmorillonite and groundwater in equilibrium with granitic rocks, the groundwater is expected to have e.g. slightly lower silica activity, set by quartz, and slightly higher potassium activity, set by muscovite or potassium feldspars. In nature, this non-equilibrium generally leads to transformation of montmorillonite to illite.

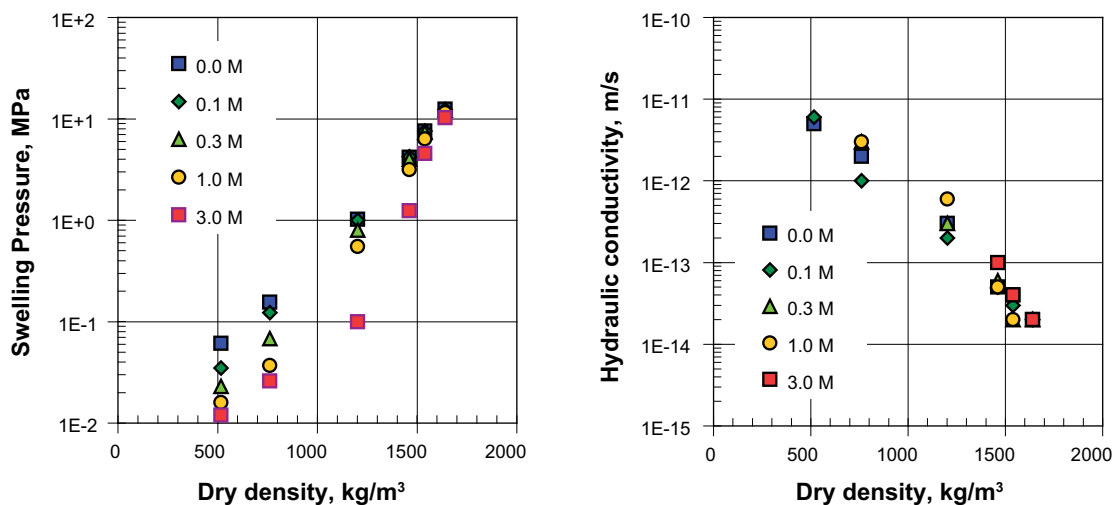


Figure 1-2. Laboratory determined swelling pressures (left) and hydraulic conductivities (right) in MX-80 bentonite at different dry densities. Legend figures indicate sodium chloride concentration in mole/liter.

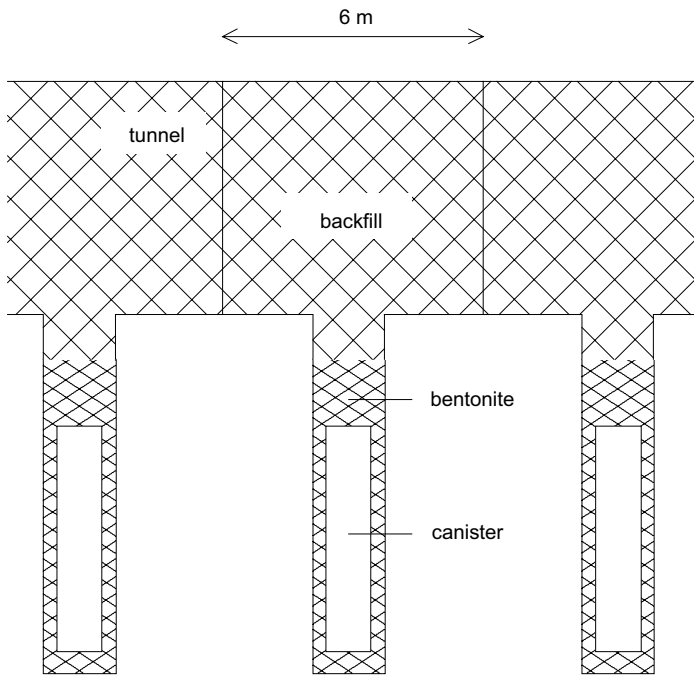


Figure 1-3. Schematic view of a section of a deposition tunnel including three canister holes in a KBS-3 repository.

The design criteria for the KBS-3 repository stipulate that the temperature should not exceed 100°C at any time or position in the buffer, including a safety margin of 10°C.

The temperature evolution has been calculated for the present repository layout to lead to a maximum temperature below 90°C, and a maximum temperature gradient below 24°C over the 0.35 m thick buffer material (Figure 1-4), /Hökmark and Fälth 2003/.

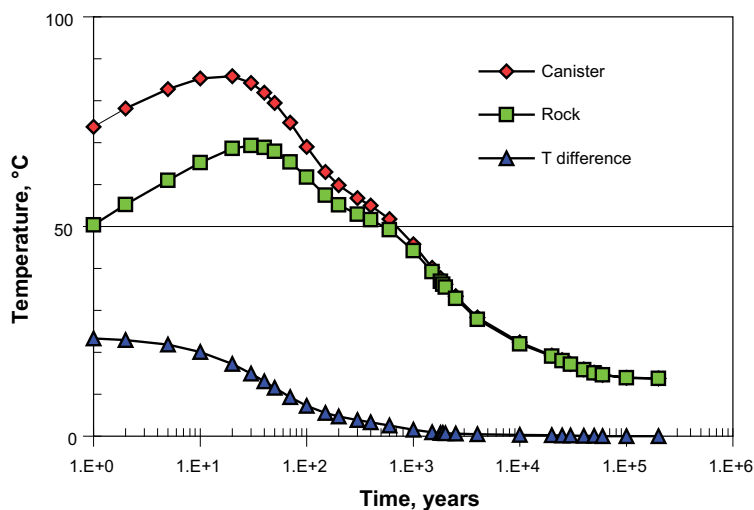


Figure 1-4. Calculated temperature evolution in a typical KBS-3 deposition hole showing the buffer temperatures at the interfaces to the canister and the rock, and the temperature gradient over the buffer. Calculated from data in /Hökmark and Fälth 2003/.

2 Montmorillonite transformation processes

2.1 General

Minerals with the same principal structure as montmorillonite but with different layer charge occur in nature. If the layer charge is near zero (pyrophyllite), there is virtually no interaction with water, which results in radically different properties than for montmorillonite. Minerals with higher layer charge and thereby more balancing cations may lead to greater interaction with water. However, the cations can be bound to the mineral surfaces and the interaction with water again ceases if the layer charge is sufficiently high. The critical layer charge for cation fixation is dependent on the properties of the charge compensating cations. Layer charges above 1.2 unit charges per $O_{20}(OH)_4$, and potassium as counter-ion may result in no water interaction and fixation of the basal distance to around 1 nm. Such a “collapsed” mineral is generally referred to as illite and the potassium fixation process is generally termed illitization. The end minerals, in which there is virtually no interaction with water, has 2 unit charges per $O_{20}(OH)_4$ for the potassium and sodium minerals (micas), and 4 units for calcium minerals (brittle micas). Figure 2-1 shows some of the 2:1 clay mineral family members and their interrelations.

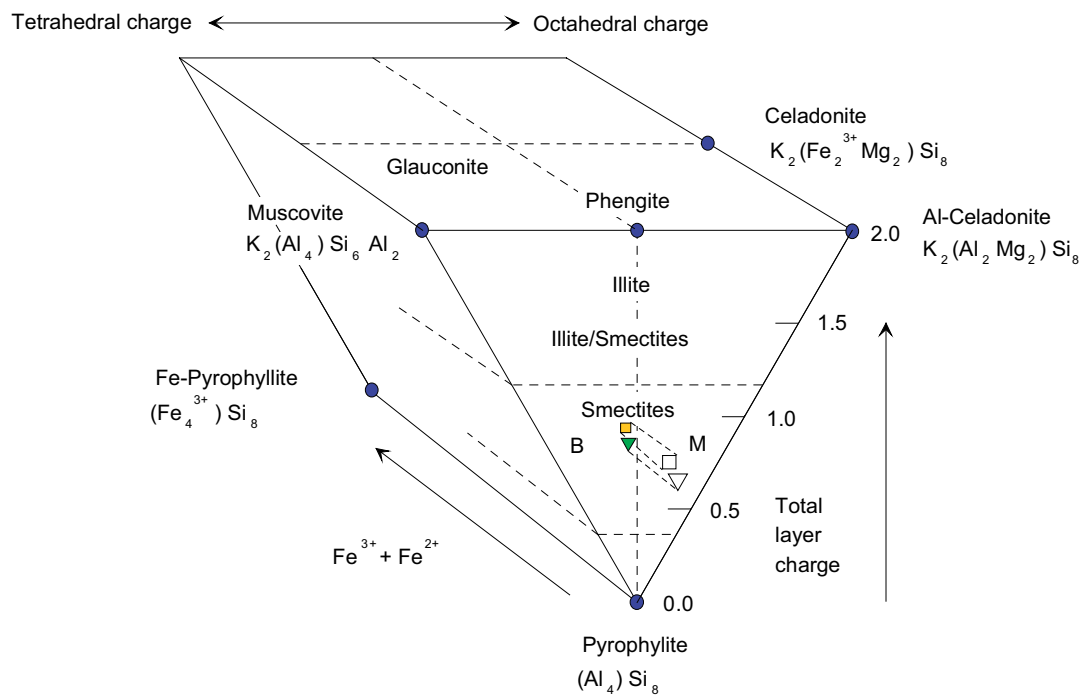


Figure 2-1. Ideal end-member minerals in the pyrophyllite – mica series with potassium as charge compensating cation, and approximate compositional ranges for illite and smectite (modified from Newman and Brown 1987/). B denotes beidellite, M denotes montmorillonite. The compositional positions of the montmorillonite minerals in the SR-CAN reference bentonite materials are indicated by a triangle (MX-80) and by a square (Deponite-CAN). All formulas are related to the basic $O_{20}(OH)_4$ cell.

2.2 Stability considerations

A starting point for quantifying the montmorillonite transformation processes is to establish stability diagrams for the involved mineral phases, i.e. ion activity ranges where these phases can coexist in thermodynamic equilibrium with an aqueous solution.

This thermodynamic treatment becomes complicated due to the inherent non-stoichiometric nature of smectite, illite etc; one is either forced to adopt a representative idealized stoichiometry which will introduce large uncertainties in the derived stability regions, or one needs a large set of equilibrium data representing the whole range of mineral compositions. A consequence is that straightforward equilibrating calculations e.g. with computer codes such as PHREEQC /Parkhurst and Appelo 1999/ becomes very cumbersome.

A more fruitful approach is to treat the mineral family as one or multiple phases of solid solutions /Garrels 1984/, /Tardy and Fritz 1981/, /Fritz 1985/. There are several indications that e.g. mixed-layered illite/smectite is mixtures of phases with smaller internal compositional variation rather than a homogeneous one-phase solid solution /Ransom and Helgeson 1993/. Nevertheless, /Aagard and Helgeson 1983/ treated the entire muscovite-pyrophyllite system as a solid solution with ideal mixing of atoms on homological sites. Using the element composition of a large number of naturally occurring minerals, the activity of the solid solution end members, particularly pyrophyllite and muscovite, was calculated. Stability field-diagrams (e.g. $\log\{H_4SiO_4\}$ vs. $\log\{K^+\}/\{H^+\}$) were then constructed by using thermodynamic data for equilibrium between these end members. An example of such a diagram is pictured in Figure 2-2.

This approach obviously produces only approximate stability fields, but it can be concluded that montmorillonite is in equilibrium only with a potassium activity below approximately 10^{-3} M at pH 7, and the equilibrium activity decreases by one order of magnitude per pH unit increase. The condition for sodium is quite different with an equilibrium activity of more than 1 M at pH 7 /Helgeson et al. 1969/.

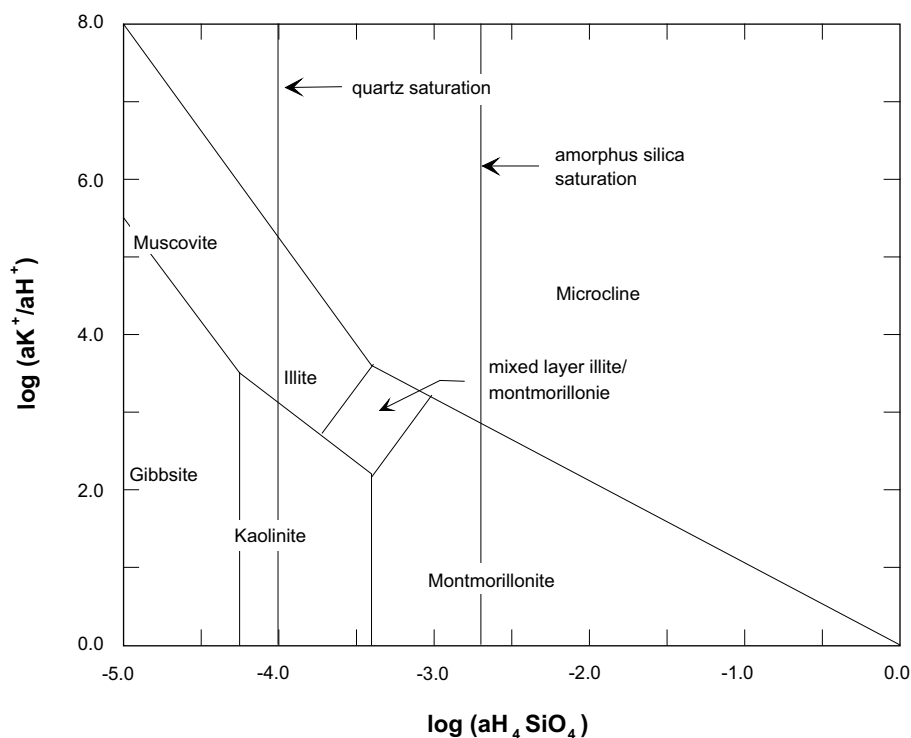


Figure 2-2. Silica mineral equilibria with the partial component potassium at 25°C. (Simplified from /Aagard and Helgeson 1983/).

A further important conclusion from Figure 2-2 is that K-montmorillonite and quartz cannot coexist in equilibrium, since the silica activity of quartz is too low. Amorphous silica, on the contrary, stabilizes montmorillonite with respect to silica activity. The conditions are again different with respect to sodium, since high charged Na-montmorillonite is stable at lower silica activities and actually may coexist with quartz.

An overarching conclusion from a thermodynamic perspective is that silica activity and potassium concentration are of major importance for the stability of montmorillonite, and if quartz can precipitate in the presence of potassium, montmorillonite will not be thermodynamically stable, and will start to transform.

2.3 Transformation processes

The typical montmorillonite transformation processes seems to preserve the 2:1-mineral structure. The reaction thus implies a path in the stability diagram directed upwards and to the left in Figure 2-2 which is also the direction found in numerous natural analogs.

The process results in a mineral with less silica and more aluminum in the tetrahedral sheets compared to the original montmorillonite. The aluminum source may be accessory minerals (e.g. feldspar) or the montmorillonite itself by congruent dissolution. The Al for Si substitution leads to a tetrahedral layer charge increase, which normally is compensated for by interlayer cations. If the charge increase progresses far enough, the electrostatic forces will eventually overcome the cation hydrating forces with a resulting interlayer collapse. Potassium has the lowest critical charge and collapsed high charged potassium montmorillonite (illite) is logically, by far, the most common transformation product. Even though a collapsed interlayer may contain some water, it is unable to expand and has obviously lost its swelling capacity.

A complete description of the involved mechanisms in the illitization process is complicated and numerous scientific articles have been published on the topic. But, the coupling between quartz precipitation and illite formation is generally found both in laboratory experiments and studies of natural systems, which may be illustrated by the study of /Abercrombie et al. 1994/, who compared pore water chemistry and the extent of illitization in oceanic and sedimentary basins, pictured in Figure 2-3.

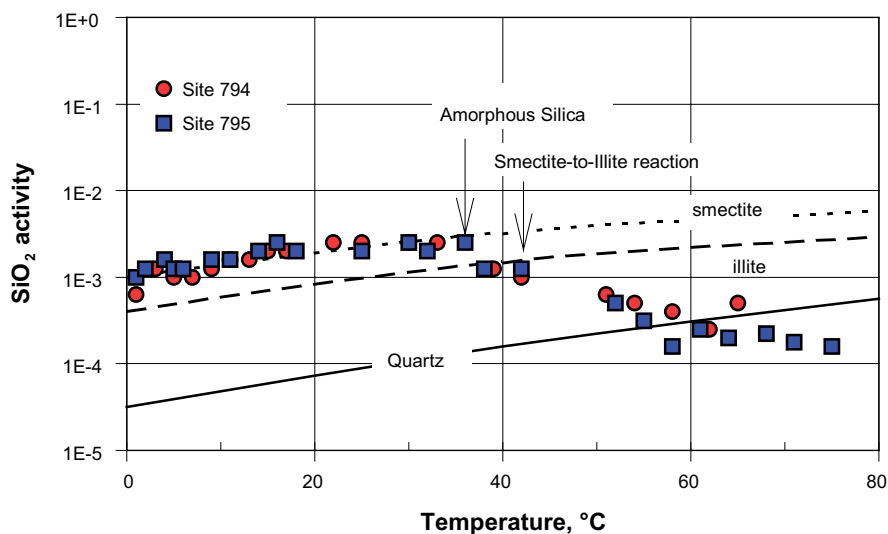


Figure 2-3. Silica activities for waters from Ocean Drilling Program sites 794 and 795 and saturation curves for amorphous silica, smectite-to-illite reaction, and quartz. Modified from /Abercrombie et al. 1994/.

The main focus in this report is on the most probable alteration scenario, which is layer charge increase and a parallel quartz precipitation, and subsequently a possible fixation of potassium. Other transformation processes are not expected to play an important role in a KBS-3 repository, since the necessary boundary conditions are intentionally avoided and not expected to arise during the lifetime of the repository. Such potential processes and related uncertainties are briefly discussed in Section 3.2.

2.4 Illitization

The term illite was introduced by /Grim et al. 1937/ for the clay-sized mica minerals found in argillaceous rocks. /Gaudette et al. 1966/ used the term for clay minerals that have a 10 Å basal repeat unit, show no evidence of inter-stratification but contain less K and more H₂O than true mica. Thus the term has been used, on one hand, in a general sense for the micaceous material in the clay-sized fraction and, on the other hand, for a specific mineral. Several authors have used the term illitic material to cover the general intention of Grim, and illite for a specific mineral.

In natural systems illitization is commonly observed. For examples, numerous investigations have shown that burial diagenesis has resulted in an illite increase with increasing depth in Gulf Coast sediments (e.g. /Burst 1959/, /Powers 1967/, /Hower et al. 1976/). This process is governed strongly both by depth (temperature) and burial rate (time). An example of typical conditions is given in Figure 2-4. Illitization has also been identified and studied in other geological contexts, such as:

- Geothermal areas, which are developed farther than what have been found in burial diagenesis /Jennings and Thompson 1986/.
- Hydrothermal zones around ore bodies, which show similar but more complex series /Horton 1985/.
- Smectite-bearing shales intruded by dikes, which yield a transition series along a line perpendicular to the surface of the dike /Lynch and Reynolds 1985/.

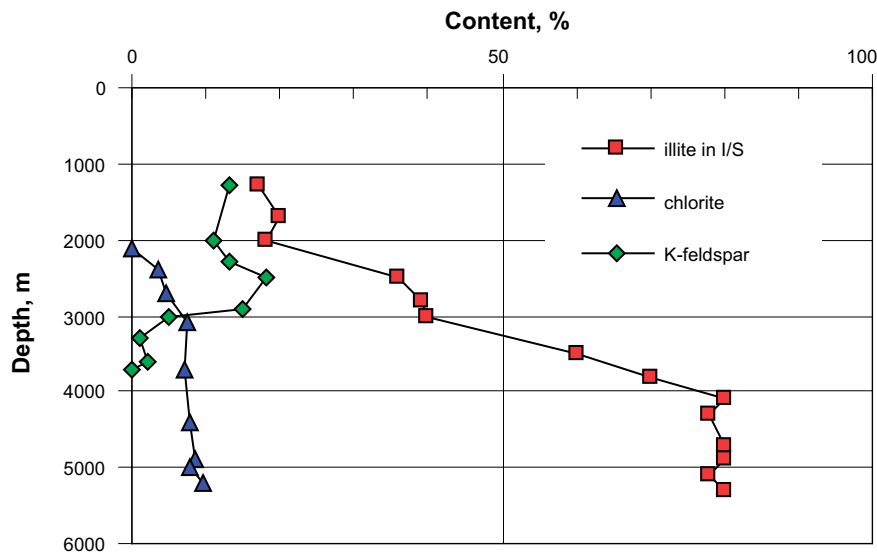


Figure 2-4. Depth-dependent changes in content of illite in smectite/illite in the <0.1 μm fraction, chlorite, and K-feldspar in the >2 μm fraction of argillaceous sediments of the early Tertiary Wilcox Group of the Gulf Coast /Hower 1981/.

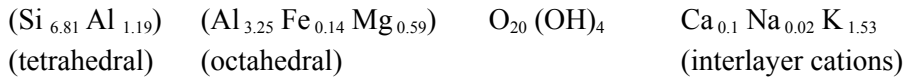
The analyses of whole rock chemistry (bulk analyses) of the sediments in the Hower study (Figure 2-4) did not show any changes in K_2O with depth, but if the $> 2 \mu m$ and $< 0.1 \mu m$ fractions were compared for K_2O it was apparent that K had been transferred from the coarser fraction to the finer (Figure 2-5). /Hower et al. 1976/ concluded that the decomposition of the K-feldspar, and perhaps detritus potassium micas, provided the necessary potassium and aluminum for the smectite to be converted to illite.

/Srodon and Eberl 1984/ suggested that the Gulf Coast sediments stopped changing at approximately 80% illite because the detritus K-bearing minerals that had been the source of potassium had been consumed (Figure 2-4 and Figure 2-6). They based their suggestions on potassium rich sediments from Poland in which the changes continued to around 90% illite. Also in the Douala basin in North Africa the change went further than what was found in the Gulf Coast sediments. Figure 2-6 also indicates the strong correlation between temperature and the illitization progression.

Beside the large number of studies concerning illitization in nature, numerous hydrothermal laboratory experiments have been made. Most of these experiments have focused on certain issues such as the effect of interlayer cations /Eberl 1978/, tetrahedral substitution /Huang and Otten 1987/, octahedral substitution /Güven and Huang 1991/, solution chemistry /Roberson and Lahann 1981/, kinetics of layer charge development /Howard and Roy 1985/, control of ordering of mixed-layers /Huang 1989/, and the effect of flow rate in flow through experiments /Kacandes et al. 1991/.

/Hower and Mowatt 1966/ made a detailed study of the structure and composition of illites and showed that many so-called illites contained interstratified smectite interlayers. A trend diagram of interlayer (K+Na) against the proportion of expandable layers showed zero percent expandable layers at 1.5 (K+Na) per $O_{20}(OH)_4$ cell.

Illite composition may be illustrated by the mineralogical composition of a natural illite from Montana, US, with less than 10% expandable layers /Hower and Mowatt 1966/



which can be compared with the composition of the montmorillonite in the MX-80 SR-CAN reference bentonite:

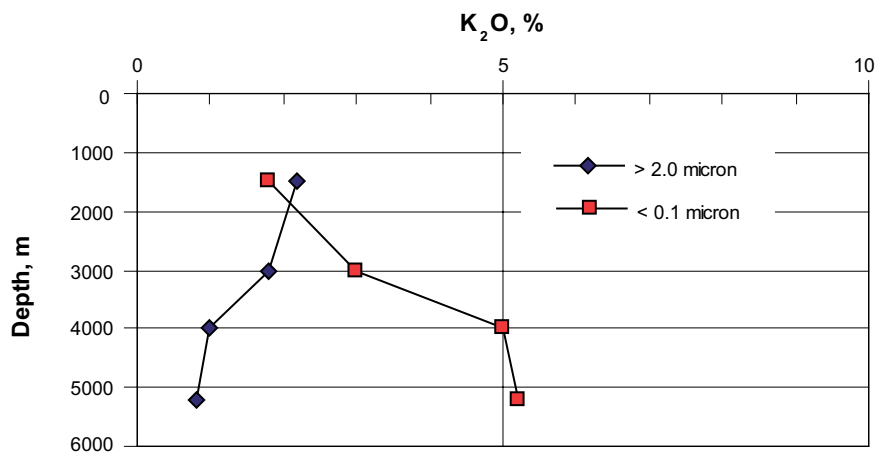


Figure 2-5. Redistribution of K_2O from the $> 2 \mu m$ fraction to $< 0.1 \mu m$ fraction as a function of depth (modified from /Hower 1981/).

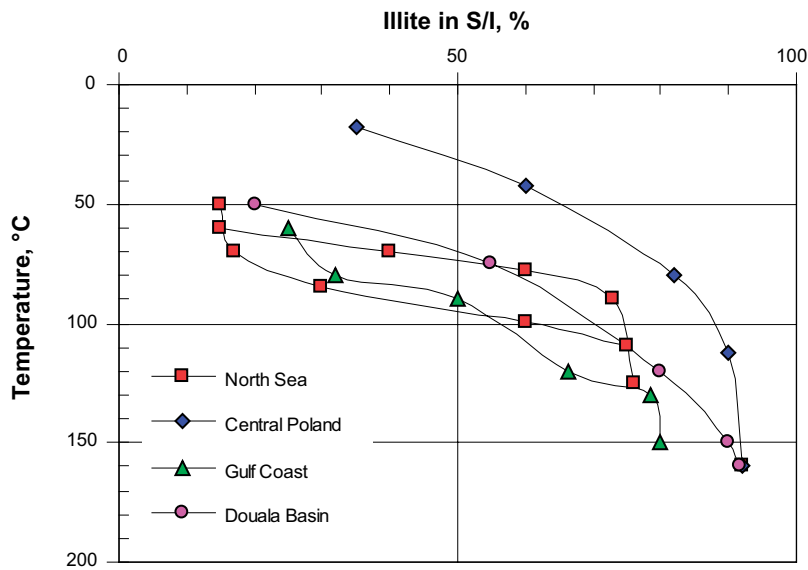
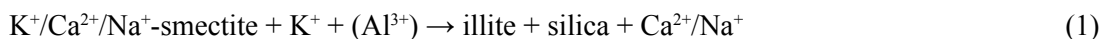


Figure 2-6. The relation between temperature and percent illite in smectite/illite in shales from different sedimentary basins. (Modified from /Srodon and Eberl 1984/.)

The main differences being that the illites have approximately one unit charge higher tetrahedral charge, and potassium as the main charge compensating cations (Figure 2-1). Simplified, the total illitization reaction may be expressed:



However, there is no general consensus concerning the exact reaction path in the transformation, and a number of explanations of the character and mechanisms of the illitization have been proposed /Moore and Reynolds 1989/. The transformation seems under certain conditions to take place without disrupting the stacks of layers, often referred to as solid state transformation (SST), and under other conditions the transformation seems to take place by a dissolution/crystallization process (DC).

/Inoue et al. 1987/ proposed the two-solid-solution model. They identified three phases in the hydrothermally altered system they studied: two are solid solutions and the other shows little variation in chemical composition. Of the two solid solutions, one varies from 100 to 50% expandable layers with random stacking. The other varies from about 50% expandable layers to pure illite, with regularly to partially ordered stacking. The first solid solution is characterized as smectite undergoing K-fixation, and the second as maturing illite. The third phase present has less than 5% expandable layers and a distinct morphology. Two different reactions for these two series were consequently proposed. K-fixation takes place as a remodeling or transformation in the flakes, whereas the laths grow because the flakes are dissolving and being re-precipitated as laths or as additions to laths (Figure 2-7).

The principle that the illitization is neither a simple alteration nor a neo-formation process but a combination of the two were supported by /Whitney and Northrop 1988/ who used analyses of the $^{18}\text{O}/^{16}\text{O}$ ratio in order to determine the reaction path. They found that a first stage produced random illite/smectite, and that approximately 65% of the oxygen was reset when illitized. In the second stage, the random and ordered illite/smectite coexisted as separate phases. In the third stage only ordered illite/smectite was produced, during which the degree of isotopic resetting was directly proportional to the degree of illitization, i.e. illite layers were 100% reset isotopically as they were formed.

/Altaner and Ylagan 1997/ argue that the SST mechanism seems to best model illitization in rock-dominated systems such as bentonite, while the DC mechanism seems to best model the illitization in fluid-dominated systems such as in the pore-space in sandstones.

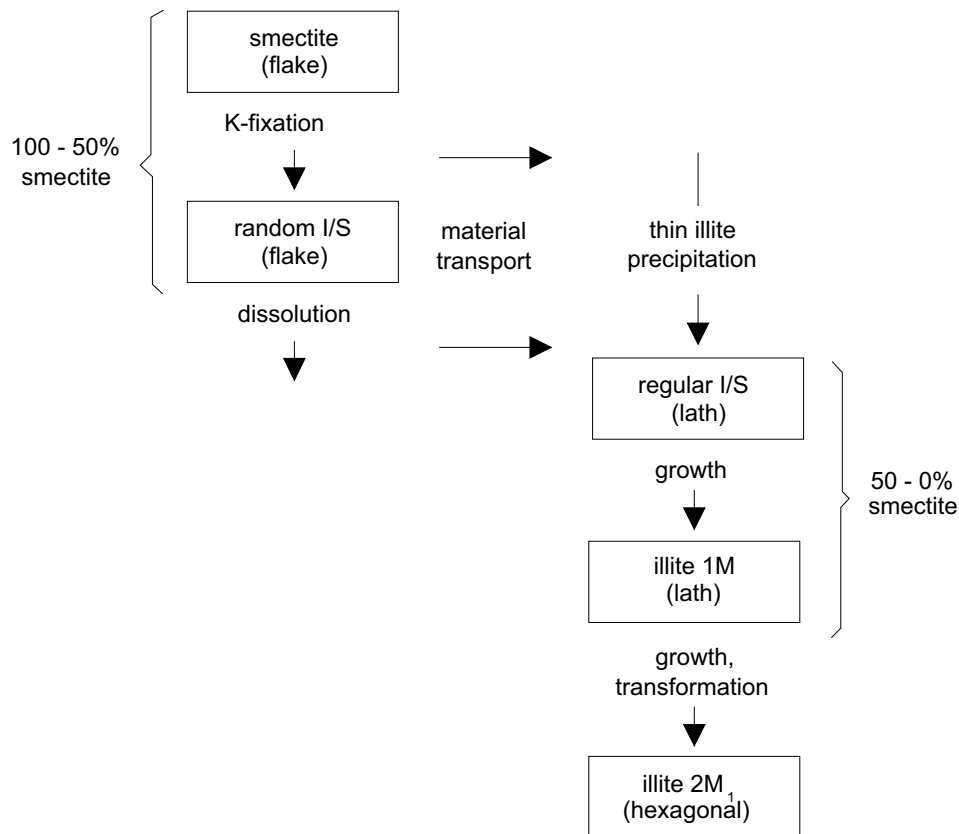


Figure 2-7. Principles of the two-solid solution illitization model. (Modified from /Inoue et al. 1987/.)

2.4.1 Kinetic models of illitization

Several investigations of illitization have been performed with the aim at obtaining a rate law for the overall transformation process. Most of these studies are based on data from geological studies of naturally occurring transformations in burial diagenesis etc. /Bethke and Altaner 1986/, /Pytte and Reynolds 1989/, /Velde and Vasseur 1992/, /Wei et al. 1993/. We are only aware of two studies based on systematic laboratory work – /Huang et al. 1993/ and /Cuadros and Linares 1996/ (in the following referred to as Huang and Cuadros, respectively).

The two laboratory based models proposed by Huang and Cuadros, respectively, together with the frequently cited field based model proposed by /Pytte and Reynolds 1989/ (in the following referred to as Pytte) are compared in the following section. The three models are summarized in Appendix 1. Common to all three is that they take into account the influence of time, temperature and K^+ -activity. None of the studies investigates potentially important factors such as aluminum availability /Boles and Franks 1979/, water ratio /Couture 1985/, /Whitney 1990/, /Karnland et al. 1994/ or silica activity /Abercrombie et al. 1994/.

The temperature dependence is included in all of the models by assuming the transformation rate to be proportional to an expression of Arrhenius type,

$$k = A e^{-E_a/RT} \quad (2)$$

where E_a is the activation energy, T the absolute temperature, R the gas constant and A is the frequency factor. For elementary chemical reactions the exponential factor in the Arrhenius expression should be interpreted as being proportional to the fraction of reactants with energy larger than or equal to E_a , while A quantifies the number of collisions per time unit of the reactants (compensated for geometrical effects). For the rate laws presented here, this interpretation might not be unambiguous, as they give the rate for the overall illitization process, which necessarily involves several more elementary steps. The details concerning the reaction

chain, or chains, is intimately connected to the structure of mixed-layered illite/smectite and is not completely resolved /Altaner and Ylagan 1997/. However, a temperature dependence of Arrhenius type seems to agree well with data.

The logarithm of equation 2 will produce a linear relationship between $\ln k$ and $1/T$

$$\ln k = \ln A - \frac{E_a}{R} \cdot \frac{1}{T} \quad (3)$$

By comparing this expression to the equation for the straight line ($y = a+bx$), the activation energy (or rather $-E_a/R$) and frequency factor corresponds to the slope and intercept of the plot of $\ln k$ versus $1/T$. This way of achieving the Arrhenius parameters is illustrated in Figure 2-8 for the case of the Huang study.

Apart from different values of the Arrhenius parameters, the models also differ in the order of the rate law, i.e. different values are adopted both for the exponents of the smectite fraction (S) and for the exponents of ion concentrations. To extract the exponent for e.g. the potassium ion concentration, the illitization rate is assumed to be proportional to

$$k' = k \cdot [K^+]^b \quad (4)$$

where k is the Arrhenius expression from above (equation 3). Taking the logarithm of equation 4

$$\ln k' = \ln k + b \ln [K^+] \quad (5)$$

gives the value of b by identifying it with the slope of the $\ln k' - \ln [K^+]$ plot as illustrated in Figure 2-9 for the Huang case.

2.4.2 Kinetic model review

When comparing the different proposed rate laws applicability for repository conditions, the following issues are of importance:

- How well does the relationship describe the test reaction.
- How well determined are the constants.
- Is the model sufficiently generally applicable in order to be used for repository conditions.

Below follows a short list of remarks on each study regarding these questions. The complete form of the different rate laws and their associated Arrhenius parameters are listed in Appendix 1.

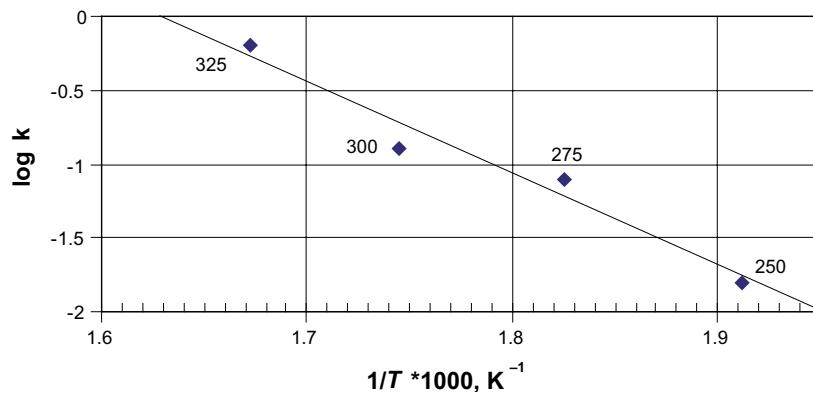


Figure 2-8. Experimental rate constants k at $[K^+] = 1 M$ versus inverse temperature (mean values for each temperature). Modified from /Huang et al. 1993/.

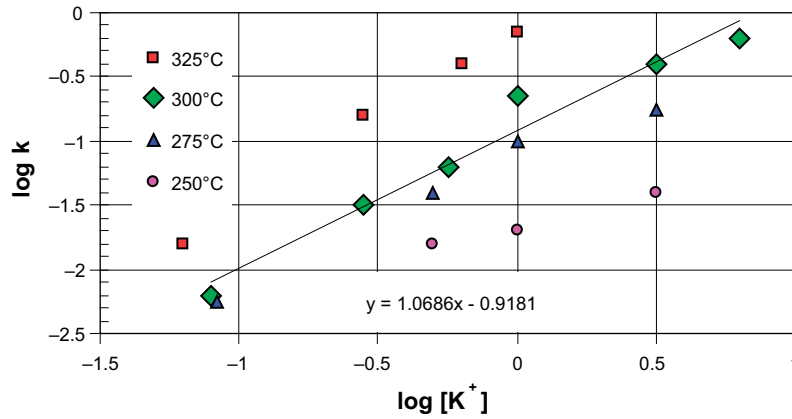


Figure 2-9. Experimental results showing the linear relationship, with slope ≈ 1 , of the logarithm of rate constant and potassium concentration at 325°C, 300°C, 275°C and 250°C. The line shows the fit to the 300°C data. Modified from /Huang et al. 1993/.

An additional test and comparison of the Huang and Pytte models (together with the model by /Velde and Vasseur 1992/) applied to a set of geological settings, is done by /Elliot and Matisoff 1996/.

The rate law of Pytte is:

$$\frac{dS}{dt} = -5.2 \cdot 10^7 \cdot e^{\frac{-16600}{T}} \frac{[K^+]}{[Na^+]} S^5 \quad (6)$$

where the $[K^+]/[Na^+]$ -ratio is set by assuming equilibrium between albite, K-feldspar and the pore water.

- The study considers the illite content of an illite/smectite profile in a contact metamorphic zone.
- The smectite fraction, S , is determined by investigating the ratio between the amount of collapsed interlayers (illite, 10 Å basal spacing) to the amount of swelling layers (smectite, larger and varying basal spacing) by X-ray diffraction (XRD).
- The transformed smectite fraction ranges from 20 to 100%.
- The thermal history of the zone is estimated by a conductive heat transport model.
- In the study a general rate expression $\frac{dS}{dt} = -kS^a \cdot \left(\frac{[K^+]}{[Na^+]} \right)^b$ is assumed and the exponents a and b are adjusted to fit measured data. Several parameter sets are claimed to give excellent agreement with the metamorphic zone data. The final choice of model parameters is made when doing additional comparisons to burial diagenesis studies. Thus, no analysis as described above seems to have been performed in order to extract model parameters.

Huang proposes a rate law of second order in S :

$$\frac{dS}{dt} = -8.1 \cdot 10^4 \cdot e^{\frac{-14100}{T}} \cdot [K^+] \cdot S^2 \quad (7)$$

- The study is based on systematic experimental investigations in dispersed systems of naturally occurring bentonite (SWy-1).
- Uses XRD for characterization of the clay in the same manner as in the Pytte study.
- Temperature, time and K^+ -concentration are controlled variables.
- To be able to handle the experiments, high temperatures (250–325°C) must be applied in order to shorten the reaction times (1–80 days).

- The transformed smectite fraction ranges from 0 to 80%.
- Influence of Na⁺, Mg²⁺ and Ca²⁺ is also investigated but to a lesser extent. The main conclusion is that these cations have a lesser influence on the illitization process but a retardation of the process is seen, especially in the case of Mg²⁺ ions.
- All parameters of the rate law are derived in the way described above.
- The rate law is tested (independently) on data from several geological settings with reasonable agreement.

The rate law in the Cuadros study leaves the smectite fraction exponent undetermined and evaluates several sets of Arrhenius parameters for different values of *a*. In the case of *a* = 5 the expression is:

$$\frac{dS}{dt} = -8.5 \cdot 10^{-7} \cdot e^{\frac{-3630}{T}} \cdot [K^+]^{0.25} \cdot S^5 \quad (8)$$

- The study is based on laboratory studies of dispersed bentonite from the Serrata de Nijar deposit, Spain.
- Temperature, time and K⁺-concentration are controlled variables.
- Makes use of the assumption that the silica concentration in solution correlates to the amount of illite produced in order to quantify the smectite fraction, *S*.
- The silica concentration measurements are claimed to be much more precise as a measurement of amount of illite produced as compared to XRD. The detection limit for illitization is thus lowered which allows lower experimental temperatures (60–200°C).
- The maximum amount of smectite transformed to illite is found to be 0.3%.
- Assumes a general rate expression $\frac{dS}{dt} = -kS^a \cdot [K^+]^b$. Parameter *b* is inferred by plotting the logarithm of the obtained rates against the logarithm of [K⁺], as described above. The *a*-parameter, on the other hand is left undetermined and several sets of Arrhenius parameters are evaluated for different values of *a*. Finally, the choice *a* = 5 is made when comparing the conversion rates to naturally occurring smectite transformation. In Table 1-1 both the model for *a* = 1 and *a* = 5 is included (named Cuadros 1 and Cuadros 5, respectively).
- The quality of the study depends critically on the amount of silica produced uniquely from the smectite-to-illite reaction. Other silicates are present in the test material and have not been accounted for to the very high degree which is necessary for the claimed precision in smectite transformation.
- Furthermore, the method heavily relies on the stoichiometry of the smectite-illite reaction in order to indirectly obtain the amount of transformed smectite via the released silica. Large uncertainties enter here both due to the intrinsic non-stoichiometric nature of the involved minerals as well as due to uncertainties regarding the composition of the neo-formed illite.
- Actually, the underlying data in the statistical treatment of the study does not contain any information on the exponent for the smectite fraction in the rate law (*a*), since it only corresponds to rates at one single point in time.

In Figure 2-10 a comparison of the three models is made for three rather different values of temperature and potassium ion concentration. Assuming an initial smectite fraction of 1, the fraction remaining as a function of time is plotted for different values of temperature and K⁺-concentration. The Na⁺-concentration in the Pytte model is here fixed for a given temperature by the van't Hoff equation, assuming equilibrium between albite and K-feldspar /Pytte and Reynolds 1989/

$$[Na^+] = 0.0135 \cdot [K^+] \cdot e^{\frac{2490}{T}} \quad (9)$$

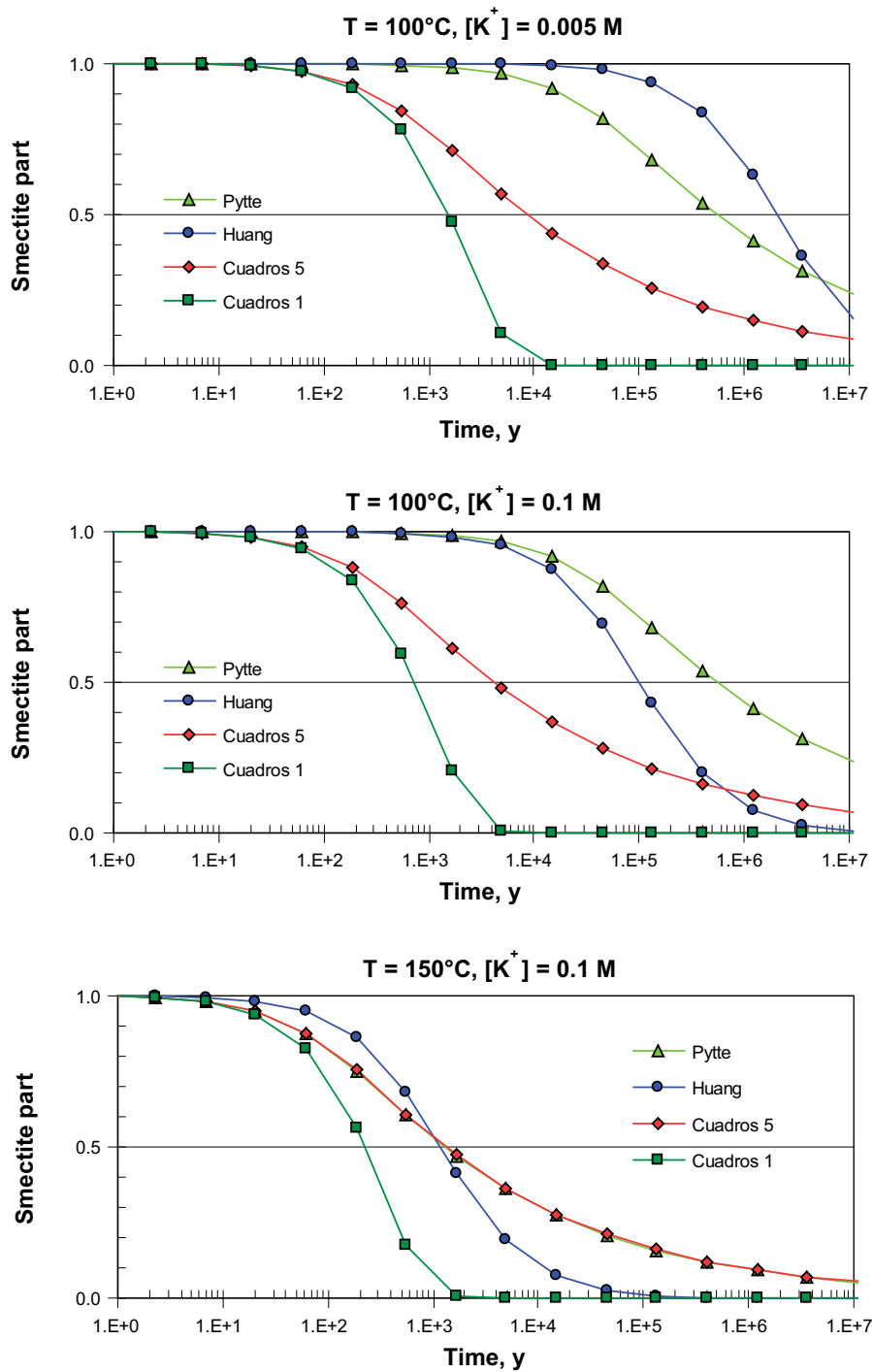
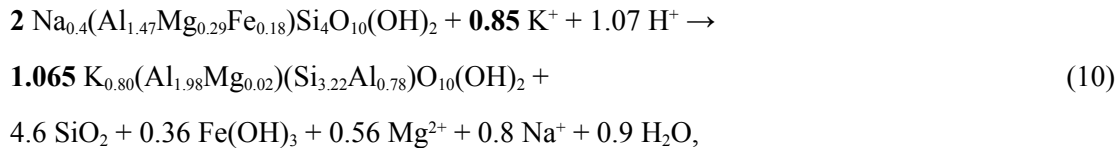


Figure 2-10. Comparison of the considered kinetic rate models for the smectite to illite transformation. Lines show the calculated remaining smectite part versus time for different temperature and potassium concentrations.

The models of Cuadros estimate a much faster alteration rate compared to the others, particularly for smaller values of [K⁺] and T (Figure 2-10). The mere fact that smectite is found to prevail in nature during much longer times gives yet another reason to question this rate law. The Huang and Pytte models predict a much slower alteration and also have a better internal agreement. The Huang profile, however, is seen to be considerably more steep which is an effect of the lower order of the Huang model ($a=2$ as compared to $a=5$).

In the following chapter the calculation of the extent of smectite transformation in a KBS-3 repository is performed based on the model of Huang. This model is considered the most generally applicable motivated by the discussion above and the following additional arguments:

- The temperature is the most critical variable, and from this aspect, a laboratory study is preferable. As an example, an increase from 170°C to 190°C, using the Arrhenius parameters from the Pytte study, will increase the rate by a factor of 5. This implies that the heat transport model in their study has to be very accurate in order to limit the uncertainties regarding e.g. peak temperatures.
- The resulting kinetic model in the Huang case is consistent with the principle of chemical kinetics, saying that the rate (at least close to equilibrium) should be proportional to the reaction quotient. Still, this statement relies on a stoichiometry,



which is based on the assumption of aluminum being conserved in the reaction as well as on the assumption that the tetrahedral layer of the neo-formed illite is compositionally similar to illite found in nature.

- The exponents for S and $[\text{K}^+]$ in the rate law of Huang are derived rather than fitted. This is done firstly by noticing a linear relationship between reaction time and the inverted smectite fraction, l/S (for fixed $[\text{K}^+]$). Furthermore, the logarithms of the slopes of these lines were plotted against the logarithm of K^+ -concentration to reveal a new linear relation with slope ≈ 1 as seen in Figure 2-9.
- In contrast, some or all of the exponents in the Pytte and Cuadros studies were adjusted to reproduce the illite profiles found in nature.

3 KBS-3 specific discussion

3.1 Quantification of possible illitization

In order to calculate the illitization by use of the Huang model, the temperature in the buffer and the potassium concentration in the pore water have to be known. Calculations of the temperature have been made for different repository geometries and material combinations, and the applicable conditions are shown in Figure 1-4. The source of potassium for a conversion has to be external, since it is possible to use almost potassium-free bentonite.

3.1.1 Potassium availability

For a typical montmorillonite structure, i.e. with the cell dimensions $a = 5.2 \text{ \AA}$, and $b = 9.0 \text{ \AA}$, the minimum charge for a complete conversion is 1.5 per $\text{O}_{20}(\text{OH})_4$ cell. This corresponds to a potassium content of $\sim 7.5\%$ of the montmorillonite mass, calculated from a typical montmorillonite formula (molar weight of 0.75 kg per $\text{O}_{20}(\text{OH})_4$ cell, section 2.4). If the montmorillonite content in the bentonite is 75% at a minimum, then potassium mass corresponding to at least 5% of the bentonite mass is required in order to fully convert the montmorillonite in the buffer. In the proposed KBS-3 concept each canister is surrounded by approximately 10.5 m^3 bentonite buffer (Figure 1-3). The buffer density $2.0 \cdot 10^3 \text{ kg/m}^3$, after saturation with water, gives a total bentonite mass of $\sim 1.7 \cdot 10^4 \text{ kg/hole}$. Consequently, a total loss of swelling ability, i.e. a complete illitization, requires approximately 850 kg of potassium per deposition hole.

The content of K-feldspar in granitic rock varies within a wide range, and no typical value can be given. Calculated from the general formula $\text{K}(\text{AlSi}_3\text{O}_8)$, K-feldspar contain 14% K by weight, i.e. 0.14% K for each percent K-feldspar in the granite. At Äspö the granodiorite is estimated to contain up to 25% K-feldspar, which gives $\sim 90 \text{ kg K per m}^3$. In order to completely transform the buffer in one deposition hole, all potassium in 9 m^3 of the Äspö granodiorite rock has to be used. It is obvious that the total amount of potassium in the vicinity of the buffer likely will be sufficient for a total transformation of the buffer. The critical question is therefore whether the potassium is available for the transformation or not.

Ground water analyses from granitic rock generally show low potassium concentration. The $[\text{K}^+]$ in the Äspö ground-water varies from a few ppm and up to 80 ppm /Nilsson 1995/. The extreme opposite is found in Salton Trough Geothermal Area where /Huang et al. 1993/ estimated the $[\text{K}^+]$ to be $3,000 \text{ ppm}$. Geochemical modeling shows that the $[\text{K}^+]$ varies within a wide range depending on the mineral assemblage, which can be divided in two major groups: one containing illite (or muscovite), kaolinite, and quartz showing a lower $[\text{K}^+]$ in the solution (e.g. $\sim 10 \text{ ppm}$ at $\text{pH } 6.5$, 40°C); and a second group containing illite (muscovite), K-feldspar (microcline), and quartz showing a higher $[\text{K}^+]$ in the solution (e.g. $\sim 900 \text{ ppm}$ at $\text{pH } 6.5$, 40°C). The equilibrium $[\text{K}^+]$ in both groups is significantly affected by pH of the pore water /Huang et al. 1993/.

The illitization rate will theoretically be higher in the warmer inner parts of the buffer at constant potassium concentration. The process will thereby consume the initial potassium, which will slow down the illitization rate, and diffusive transport of potassium will be initiated by the resulting concentration gradient. The potassium distribution around the buffer and diffusive transport of potassium through the buffer have been discussed and modeled by /Hökmark 1995/. The conclusion was that the diffusive transport through the bentonite will strongly reduce the illitization of the buffer under relevant repository conditions. Consequently, the following calculations overestimate the degree of illitization since a constant potassium concentration is used and the transport restriction in fractures and buffer is not taken into account.

3.1.2 Illitization modeling results

Results from calculations by use of the Huang model are shown in Figure 3-1. The calculations use the constants for frequency factor (A) and activation energy (E_a) determined in laboratory experiments by Huang et al. and the maximum potassium concentration measured at Äspö, and therefore represents best available realistic data. The maximum temperature in the repository is calculated to be below 50°C after 1,000 years, below 25°C after 10,000 years and less than one degree above the unaffected rock temperature after 100,000 years. Obviously, the calculated montmorillonite illitization is insignificant for the actual KBS-3 conditions and the margins are very large. The crucial question is consequently if there are any major weak points in the model calculations.

3.1.3 Calculation uncertainties

The relevance of the model calculations are dependent on the validity of the expression for repository conditions, the correctness of constants, the correctness of input variables, and of course, if there are other alteration processes which are more important.

Model applicability

The correctness in extrapolation from high temperature laboratory conditions to the significantly lower temperature in the repository is not self-evident, since the exact transformation mechanism is not clear.

Quartz crystallization is kinetically prohibited at low temperatures. If the kinetics of quartz really is the governing reaction in the illitization process, then the lack of quartz crystallization at low temperature implies that the montmorillonite alteration will be overestimated by the extrapolation, especially at the temperature conditions in the later stage of the thermal phase.

There are indications that different reaction mechanisms regarding the transformation are involved, or are relatively more dominant, in different water ratio regions /Couture 1985/, /Whitney 1990/, /Altaner and Ylagan 1997/. Compared with KBS-3 conditions the Huang experiment is more hydrothermal in character as it is performed at a water ratio of 10. However, the model is validated against natural analogs, which have much lower water ratios.

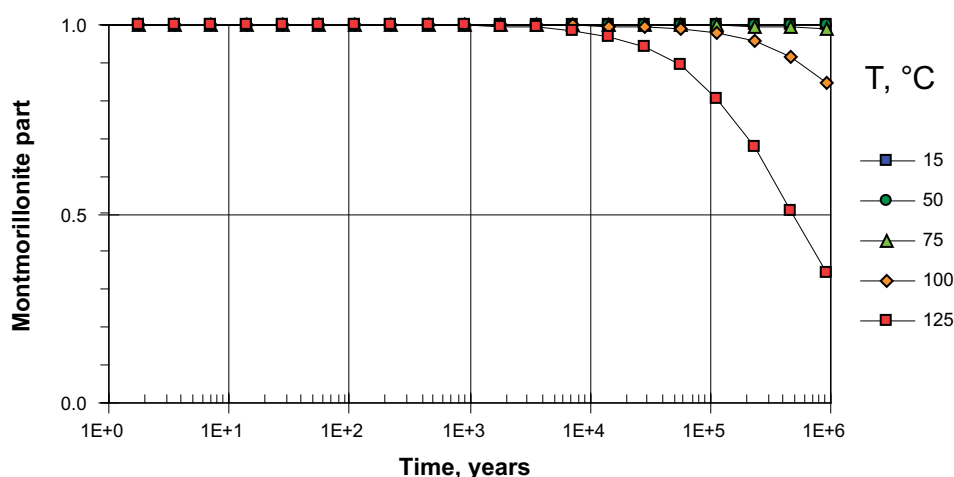


Figure 3-1. Remaining montmorillonite part for different temperatures in a hydrothermal system with $[K^+] = 0.002$ mole/liter (80 ppm) according to the Huang et al. kinetic model and laboratory determined constants ($E_a = 28$ kcal/mole and $A = 8.1 \cdot 10^4 s^{-1} mole^{-1}$).

/Eberl et al. 1993/ showed in laboratory tests that illite may be formed from smectite under hyper-alkaline conditions at temperatures as low as 35°C. /Bauer et al. 2005/ observed a distinct illite peak after 230 days in hydrothermal tests at 80°C and 1 M KOH solution. The illitization rate is consequently dramatically increased at very high pH conditions. The illitization rate at the KBS-3 design criterion pH 11 is not determined and an obvious uncertainty. However, the solubility of silica begins to increase significantly with pH at pH 9, and a further stronger increase is induced at pH 11 (Figure 3-3). Consequently, the solubility of montmorillonite is several orders of magnitude higher at pH 14 compared to pH 11, which is expected to also reflect the illitization rate difference, see section 3.2.3.

Model constants

The constants A and E_a are uniquely determined by well established experimental techniques. A drawback is, though, the use of XRD for illite quantification since the accuracy is rather low. However, this is not expected to significantly influence the inferred activation energy, but a systematic underestimation of the frequency factor cannot be excluded.

Input variables; temperature and potassium content

The temperature evolution in the buffer is probably the best predicted variable of all since it is based on fundamental principles and well determined properties. Further, the margins with respect to increased temperature duration are large, and less than 20% of the montmorillonite is calculated to transform even if the maximum temperature of 100°C prevails during the entire lifetime of the repository.

The potassium concentration may vary significantly for natural reasons and will be affected by temperature and pH in the groundwater. The maximum pH effect will be if the pH is set by potassium ions from e.g. cement. The design criteria of pH 11 thereby give the maximum potassium activity 1 mM, which is less than the measured maximum value at Äspö. The salinity in seawater is 3.5% by weight, and the potassium concentration is around 400 ppm (~10 mM) and the sodium concentration is 10,800 ppm (~470 mM). The extreme value of 3,000 ppm (~80 mM) mentioned above speeds up the illitization rate by a factor of 40, which still gives insignificant illitization in the repository. Extreme water saturation scenarios may theoretically lead to very high local concentrations, due to evaporations in the warm parts and subsequent condensation in the upper less warm parts of the buffer. However, possible high concentrations will be reduced by diffusive transport after full water saturation. The enrichment process has been looked for in the LOT experiment at Äspö /Karnland et al. 2000/, but no clear evidence for this type of increased porewater concentration has been found.

3.2 Other possible alteration processes

3.2.1 Chloritization

Chlorites have the same basic structure as montmorillonite, but the layer charge is normally close to 2 unit charges per $O_{20}(OH)_4$. The layer charge is balanced by positively charged, octahedrally coordinated, hydroxide sheets. The central ion in the interlayer hydroxide sheet may be any di- or tri-valent metal ion, normally Mg, Al or Fe.

Transformation from montmorillonite to chlorite is occasionally found parallel to illitization (Figure 2-4). The formation of chlorite has been explained as a consequence of illitization in an authigenic process similar to the crystallization of quartz /Niu et al. 2000/. It cannot be excluded that chlorite may be formed from montmorillonite without illitization in the lack of potassium and in access to Mg, Fe or Al, or as a direct transformation at high temperature and pH. However, there are no indications that this process should be faster than the illitization process at repository conditions.

3.2.2 Fixation of other ions than potassium

Brammallite and rectorite may be seen as a sodium equivalent to illite and illite/smectite. The mean layer charge is higher than in illite, normally close to 2 unit charges per $O_{20}(OH)_4$ cell. Transformation of montmorillonite into brammallite/rectorite is theoretically possible if potassium is not available, and release of silica from the montmorillonite continues until the required tetrahedral charge is reached. Both brammallite and rectorite are much less commonly found as alteration products of montmorillonite in natural sediments compared to illites.

The critical layer charge for collapse of montmorillonite to a non-swelling mineral depends on the cation. /Eberl 1980/ proposed a general formula to indicate the expandability of 2:1 layer structures. He used the concept of an "equivalent anionic radius", of the 2:1 layer, r_a , to calculate the upper charge limit for expandability according to

$$C_c = \frac{A}{4\pi \cdot r_a} \quad (11)$$

where C_c is the critical charge for collapse per $O_{20}(OH)_4$ formula unit, and $A = a \cdot b \text{ \AA}^2$, where a and b are the cell dimensions in \AA . For K- and Na-clays in water, these are $C_K = 0.0329 A$ and $C_{Na} = 0.0366 A$. Consequently, 2:1 layer silicates with interlayer Na would continue to expand at a layer charge at which that with interlayer K would not, and trioctahedral varieties should expand at larger layer charge than dioctahedral. The minimum mean layer charge for full potassium fixation is 1.5 unit charges, and a sodium analog would consequently have a mean layer charge of at least 1.7 unit charges for the same cell dimensions.

Consequently, high charge montmorillonite may be formed by the same process as illitization if sodium is available and potassium is not. The alteration would not be detected by standard XRD methods since the interlayers in the altered montmorillonite still expand. The produced high charged montmorillonite will consequently have swelling properties and may serve well in the buffer. However, a possible risk is a subsequent ion exchange, of which potassium is the most critical. The supply of potassium thereby has to be considered for the whole repository lifetime and not only during the thermal phase.

Fortunately, there are no obvious indications that the layer charge increase is faster in lack of potassium, rather on the contrary, but no specific studies of charge increase rates as a function of ion type have been found.

Assuming the charge increase rates are the same for potassium and sodium we can calculate the layer charge increase by the Huang model. In order to ensure that the charge increase is not underestimated we can use the KBS-3 design criterion for maximum salinity (3 M). The calculated results (Figure 3-2) show that less than 20% of the montmorillonite will be transformed also at these very pessimistic assumptions with respect to rate and concentration.

3.2.3 Silica release due to high pH

The silica solubility increases significantly at pH above 9 due to the possibility for the H_4SiO_4 -specie to lose one or two of its protons. The total equilibrium SiO_2 -concentration ($[H_4SiO_4] + [H_3SiO_4^-] + [H_2SiO_4^{2-}]$) is given by the law of mass action

$$[SiO_2]_{TOT} \approx \{H_4SiO_4\} (1 + K_1/\{H^+\} + K_1K_2/\{H^+\}^2) \quad (12)$$

where $K_1 = 10^{-9.9}$ and $K_2 = 10^{-11.7}$ denotes the equilibrium constants for the dissociation reactions. The total SiO_2 -concentration as a function of pH is shown in Figure 3-3, assuming an H_4SiO_4 -activity for saturated amorphous silica.

The tetrahedral silica in the montmorillonite consequently equilibrates at higher concentrations at pH over 9. Diffusive removal of silica or precipitation of new silica minerals thereby lead to a faster increase of the tetrahedral layer charge compared to near neutral conditions. The corresponding increase in concentration of charge compensating cation leads to a change in the

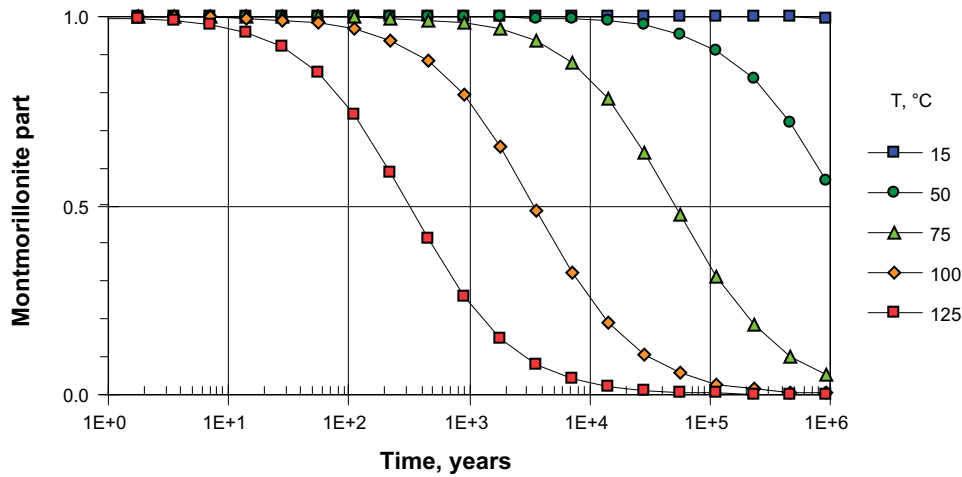


Figure 3-2. Remaining montmorillonite part for different temperatures in a hydrothermal system with $[Na^+] = 3$ mole/L assuming that the Huang et al. kinetic model and laboratory determined constants ($E_a = 28$ kcal/mole and $A = 8.1 \cdot 10^4$) for potassium is valid for also for the formation of sodium high charge montmorillonite.

interaction with water and thereby to a change in sealing properties. The layer charge may reach the critical value for collapse, which results in total loss of expandability and in principle, to the same consequences as for illitization. Eventually, the process may lead to a general dissolution of the montmorillonite /ECOCLAY II/, /Karland et al. 2005/.

At pH 11, which is set as the KBS-3 design criterion, the divalent anion $H_2SiO_4^{2-}$ starts to play an important role leading to a dramatic increase in silica solubility. At pH 11 the total silica concentration are calculated to be approximately 16 times larger compared to neutral pH conditions, and at pH 12.4, representing matured Portland cement, the theoretical increase in total silica solubility is more than 3 orders of magnitude larger than at near neutral conditions.

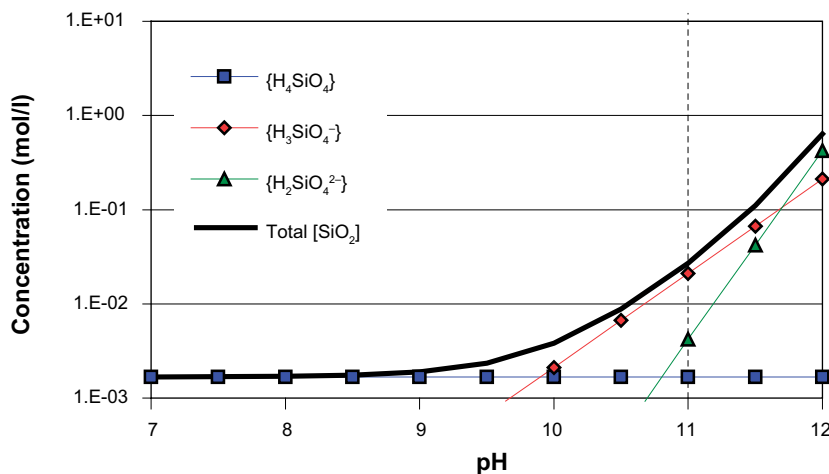


Figure 3-3. Total concentration of silica as a function of pH assuming H_4SiO_4 -activity for saturated amorphous silica at 25°C. At pH=9.9 the $H_3SiO_4^-$ starts to dominate and above pH=11.7 $H_2SiO_4^{2-}$ dominates. The upper limit for the KBS-3 design criterion, pH=11, is indicated.

The total silica concentration difference between the bentonite porewater and the groundwater increases approximately by the same factor, assuming the groundwater in equilibrium with quartz. This leads to diffusional transport of silica from the bentonite into the groundwater. Besides the difference in equilibrium concentration, the limiting factors for this mass loss will likely be the contact area between the buffer and the groundwater, and the groundwater flow, since the kinetics of the montmorillonite dissolution is relatively fast /Bauer and Berger 1998, Huertas et al. 2001, Sato et al. 2005, Karnland et al. 2005/.

3.2.4 Temperature gradient induced silica release and transport

The temperature gradient over the buffer (Figure 1-4) induces a silica concentration gradient within the buffer. The corresponding calculated diffusive flux and accumulated silica transport is plotted in Figure 3-4. The calculation is made by assuming an effective diffusion constant (D_e) of the dissolved silica of 10^{-10} m²/s, a porosity of 0.43 and a plane geometry of the buffer. The silica concentration gradient is calculated by PHREEQC /Parkhurst and Appelo 1999/ by assuming a silica solution in equilibrium with amorphous silica at the actual temperatures shown in Figure 1-4.

The silica transport is seen to proceed up to at least 50,000 years, but the final value of the accumulated SiO₂ (3.3 mol/m²) corresponds to a mass loss of only 0.05%, assuming a dehydrated bentonite mass of 10⁴ kg and a rock-buffer interface area of 20 m² for the canister section of the buffer. Thus, the buffer density change due to this effect will be completely negligible.

The effect of the silica transport on the layer charge increasing reactions is estimated in the following way. The montmorillonite crystal unit cell in MX-80 has a mean layer charge of 0.64 and consequently needs a charge increase of 0.56 to reach the critical value (1.2) where layer collapse is possible in conjunction with potassium. The molecular weight of the O₂₀(OH)₄ cell of the montmorillonite in MX-80 is 0.75 kg/mol. Assuming 80% montmorillonite in the bentonite and a total mass and area as above, a corresponding critically charged zone width is consequently:

$$0.35 \text{ m} \cdot \frac{1}{0.8} \cdot 20 \text{ m}^2 \cdot \frac{3.3}{0.56} \text{ mol/m}^2 \cdot 0.75 \text{ kg/mol} = 0.004 \text{ m}$$

$$\frac{10^4 \text{ kg}}{10^4 \text{ kg}} = 0.004 \text{ m}$$

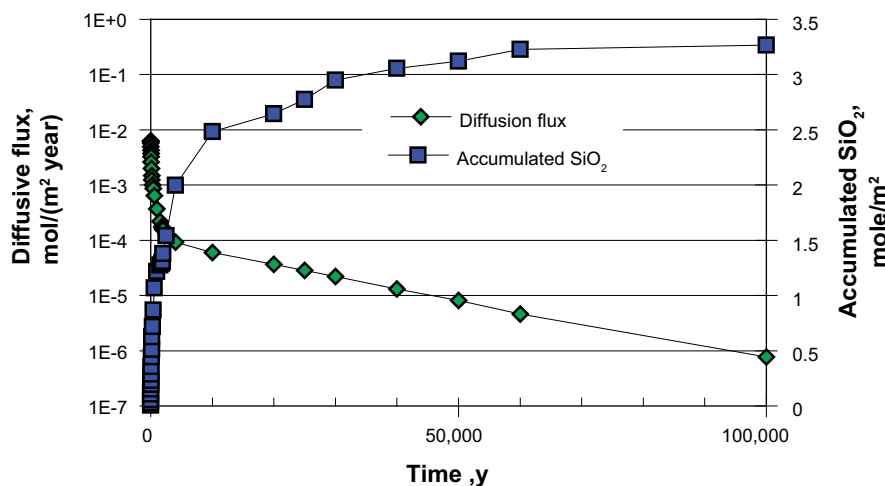


Figure 3-4. Silica diffusive flux and accumulated transported silica under pH neutral conditions due to the actual thermal gradient present in the repository (Figure 1-4). The calculation uses an effective diffusion constant $D_e=10^{-10}$ m²/s and a porosity of 0.43.

The transported silica could also contribute to a lowering of the buffer performance by precipitation/cementation in the outer cooler parts. This effect is estimated by calculating the total mass increase in the outer 5 cm of the buffer (arbitrarily chosen) under the assumption that all transported silica precipitates there. This mass increase is consequently equal to $7 \cdot 0.05\% = 0.35\%$ (where 0.05% is the total mass loss from above).

In conclusion, the layer charge increase due to diffusional silica transport at neutral pH conditions corresponds to a critically charged zone of approximately 4 mm and a cementation effect of 0.35% mass increase in a 5 cm zone. Obviously, at neutral pH conditions both effects are very small and can be neglected (Figure 3-5).

At pH 11, the limiting KBS-3 design criterion, the 16 times higher silica solubility compared to neutral conditions leads to a critically charged montmorillonite zone of 6.2 cm and a silica precipitation of 4.4% by weight in the outermost 5 cm. Such effects cannot be neglected, but they likely are overestimated since the calculations are based on $D_e = 10^{-10} \text{ m}^2/\text{s}$. At pH 11 the anion H_3SiO_4^- is dominant and a more probable value is $D_e = 10^{-11} \text{ m}^2/\text{s}$ /Ochs and Talerico 2004/ which also lowers the calculated values by one order of magnitude.

3.2.5 Redox-reaction induced octahedral layer changes

The octahedral layer in montmorillonite frequently contains a significant amount of iron which may change oxidation state. Normally, the iron is in a maximum oxidized condition in commercial material due to exposure to air during mining and handling. In the presence of an electron donor the structural Fe(III) in the octahedral layer may reduce to Fe(II). Such redox reactions in montmorillonite are generally fast, and there are no relevant kinetic restrictions for the transformation in a KBS-3 repository /Stucki et al. 1984/. A reduction leads to an increase of the total layer charge, and a potential risk for fixation of interlayer cations if the charge change is large enough. The magnitude of the possible alteration due to reduction of structural iron is restricted by the iron content in the montmorillonite and the presence of an electron donor. The large amount of metallic iron in the canister insert makes a complete reduction of octahedral iron possible. The SR-Can reference bentonites contain 0.37 Fe (MX-80) and 0.45 Fe (Deponit CA-N) per $\text{O}_{20}(\text{OH})_4$ cell, and the corresponding maximum possible layer charge increases are consequently significant, but not sufficient for fixation of potassium. Further, the effect of such octahedral layer change is expected to have less effect compared to a similar charge change in the tetrahedral layer /Sato et al. 1992/, /Sposito et al. 1999/.

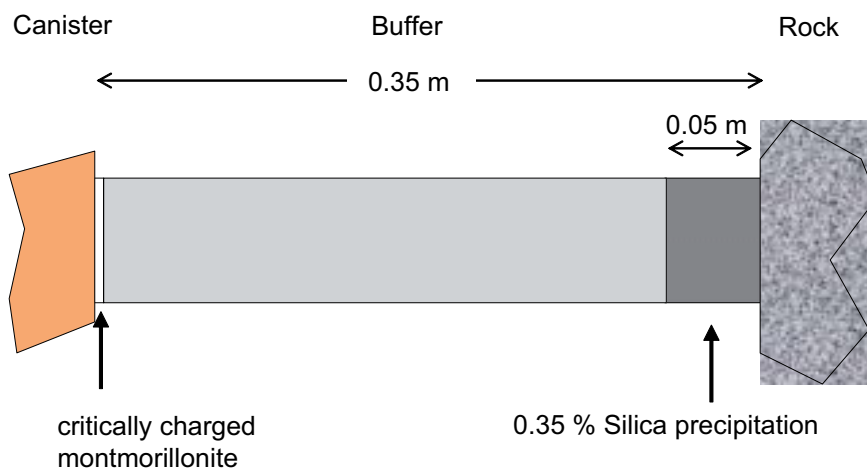


Figure 3-5. Cross section of the 0.35 m buffer illustrating the calculated maximum effect of silica diffusion, at pH neutral conditions, as a result of a temperature gradient over the buffer.

Recent laboratory experiments at KBS-3 repository temperatures conditions have shown that reactions between montmorillonite and metallic iron in an oxygen free environment may be relatively fast and in some cases also lead to a general breakdown of the montmorillonite structure /Lantenois et al. 2005/. The effects of such reactions on an KBS-3 buffer are not possible to foresee at the present stage, but the effects are likely limited by the spatial conditions in combination with transport restrictions due to the low solubility of the iron species. A decisive question for the potential extent of transformation is if the reduction may be induced by hydrogen gas released from the oxidizing iron specie or, if the reduction of octahedral iron only takes place in the vicinity of an oxidizing iron source.

Dissolution of montmorillonite and precipitation of other iron rich minerals are thermodynamically possible and has been verified in laboratory experiments. Berthierine has been found where the partial pressure of oxygen exceeds magnetite equilibrium, and formation of Fe-saponites is expected if oxygen pressure is significantly lower than magnetite-hematite equilibrium. Both types of mineral formation have been experimentally verified, but only in long term experiments at 250°C /Wilson et al. 2006/.

3.2.6 Temperature induced octahedral layer charge changes

At temperatures above 700°C there are re-crystallization processes which lead to completely new phases. Temperatures above 400°C involve de-hydroxylation and the formation of quasi-stable phases. The mineral structure is radically changed and no swelling properties are preserved. The involved processes cannot take place at significantly lower temperatures and may not be considered at repository conditions.

Small interlayer ions appear to be capable of moving into the layer structure and change the octahedral layer charge at temperatures between 200 and 400°C /Hoffmann and Klemen 1950/, /Greene-Kelly 1953/. The reaction is irreversible and the montmorillonite lose its ion-exchange capacity and swelling properties. The process is used in clay analyses to quantify the octahedral layer charge by neutralization with lithium or magnesium ions. The critical temperature for penetration is ion-type dependant, and in the case of lithium, 250°C is recommended for 24 h. The reaction is obviously relatively fast also at this moderate temperature, and a crucial question is if the process may take place at lower temperatures, and if so, at what rate. The reaction involves dehydration, which likely will reduce the reaction rate significantly under repository conditions.

3.3 Effects of montmorillonite alteration

3.3.1 General

A montmorillonite transformation may take place generally in the buffer or localized as a consequence of e.g. temperature or potassium distribution. However, the hydro-mechanical properties of the buffer will partly distribute the water to the remaining expandable interlayer, i.e. the unaltered parts will swell and the altered parts will be consolidated. The difference between localized and general transformation is not possible to fully model since the rheological properties of the transformed material is not known. Consequently, a transformation has to be treated as general in a performance assessment perspective since this would lead to the largest reduction in sealing properties.

Porosity changes are often discussed in geochemical modeling since a porosity decrease is expected to lead to reduced transport capacity. In montmorillonite, this is partly true with respect to diffusive transport, but may not at all be true with respect to advective transport. In the case of a KBS-3 buffer, the initial porosity is 43% and the hydraulic conductivity is below 10^{-13} m/s, which is compatible with fracture free granite with a porosity of much less than 1%.

The low hydraulic conductivity in montmorillonite is consequently mainly not an effect of low porosity, but of the interaction between the interlayer cations and water. Montmorillonite alteration to a mineral with lower density will indeed reduce the total porosity, but the interlayer distance in the remaining montmorillonite will after all increase as long as the neo-formed mineral has higher density than the mean bulk density of the water/mineral system. Since such low density minerals are not realistically formed, reduced porosity will not play an important role in the sealing capacity if the montmorillonite is altered to a non-swelling mineral. On the contrary, the hydraulic conductivity may increase several orders of magnitude if a substantial part of the montmorillonite is transformed, even if the porosity is reduced.

3.3.2 Minor layer charge changes

A minor general change in layer charge will in principle change swelling pressure and hydraulic conductivity in a way which is characteristic for the new mean layer charge. However, if the layer charge change takes place by silica release, then precipitating silicates may lead to a deterioration of the rheological properties of the buffer material.

3.3.3 Illitization

The effects are quite different in case of illitization since the process induces local interlayer space collapse and the previously bound water is released. The remaining expandable interlayer will thereby incorporate the released water and expand in a corresponding way. The process simply leads to a lowering of the montmorillonite content. A fifty percent illitization will result principally in a doubling of the expandable layer distance, which leads to a significant change in swelling pressure and hydraulic conductivity. The KBS-3 design criterion for minimum swelling pressure is 1 MPa, which corresponds to a calculated maximum acceptable montmorillonite illitization of 30%. The hydration principle is shown in Figure 3-6, and the calculated changes in swelling pressure are shown in Figure 3-7.

The increase in layer charge is due to silica release, which likely will precipitate and deteriorate the rheological properties of the buffer material. The effects can only be estimated since the character and distribution of precipitates are not well known.

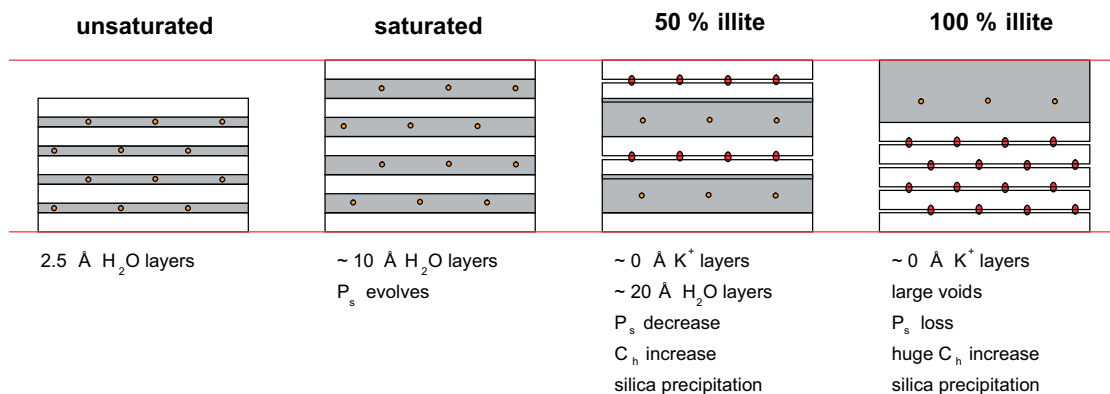


Figure 3-6. Cartoon of water conditions in the montmorillonite interlayer. P_s indicate swelling pressure and C_h indicate hydraulic conductivity. Unsaturated conditions (left) show the initial low degree of hydration at buffer placement. Saturated conditions show the maximum cation hydration in a limited space. 50% illite shows the collapsed interlayers and non-collapsed layers further hydrated. 100% illite shows the totally collapsed interlayers and large voids over which no force interaction with the surroundings particles exist.

3.3.4 Chloritization

In the case of chloritization the effects are similar to illitization, but less pronounced since the neo-formed octahedral interlayers have a spacing of around 4.5 Å. A fifty percent chloritization consequently results in an approximately 50% volume increase of the remaining expandable interlayers, i.e. approximately half the effect of illitization.

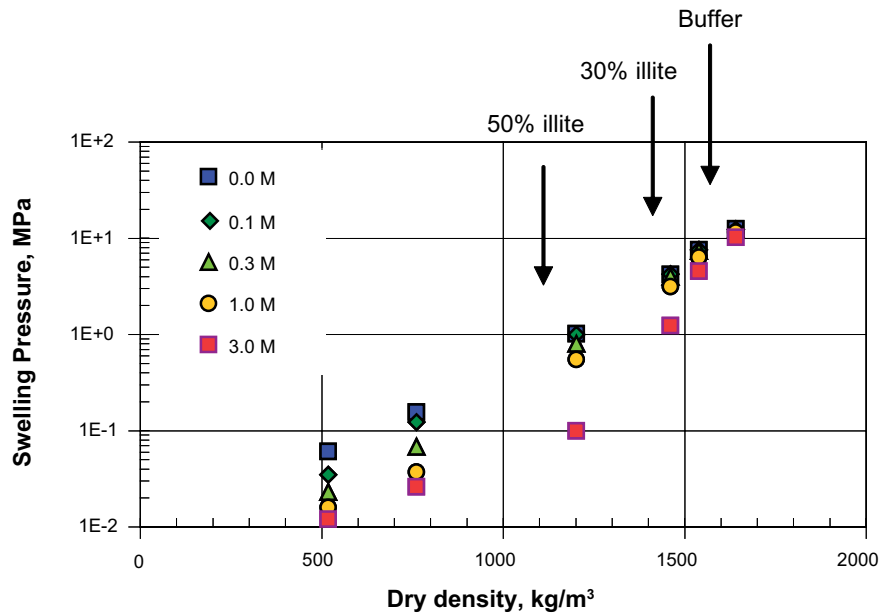
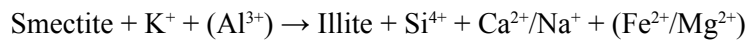


Figure 3-7. Swelling pressure of MX-80 material in contact with pure water and NaCl solutions. Dots show measured values. Buffer indicates the swelling pressure of unaltered buffer material at KBS-3 target density, 30% illite indicates the pressure at maximum acceptable transformation, and 50% illite illustrates the pressure at a 50% illitization.

4 Summary and conclusions

The conditions in a KBS-3 repository are in many respects similar to those in many natural smectite formations. Such conditions are: full water saturation, high solid to water ratio, limited interaction with external groundwater and elevated temperature. In these formations, the smectite minerals are slowly transformed into mainly illite if potassium is available. The process is accompanied by crystallization of quartz and sometimes of chlorite. The illitization may take place by silica release without disrupting the montmorillonite layer structure, or by dissolution of the montmorillonite and subsequent crystallization of illite. In the first case, the release of silica leads to a layer charge increase, which initially results in improved sealing properties. However, reaching layer charges above 1.2 per $O_{20}(OH)_4$ cell, potassium will be fixed and the interlayer water structure collapses and the sealing properties are successively lost. The general reaction in both cases may be expressed:



The same general process has repeatedly been observed in laboratory experiments, and the illitization has been concluded to take place due to the thermodynamic non-equilibrium between the smectite mineral and the porewater with respect to silica and potassium activities, respectively. Therefore, it is most likely that illitization will take place also in a repository, and since this leads to a loss in sealing properties it is of vital importance to determine the extent of the montmorillonite transformation. Several reports on the kinetics of the smectite to illite reaction have been published, and the rate expressions basically have the same form

$$\frac{dS}{dt} = -A \cdot e^{-\frac{E_a}{RT}} \cdot S^a \cdot [K^+]^b,$$

but differs significantly in the values of the parameters A , E_a , a and b . Three models, proposed by /Pytte and Reynolds 1989/, /Huang et al. 1993/ and /Cuadros et al. 1996/, respectively, have been compared, and the following observations are made:

- The Huang study determines the set of parameters independently and uniquely by systematic investigations of the transformation process with respect to temperature, time and potassium ion concentration.
- The inferred model of Huang was tested independently on geological settings with reasonable agreement.
- Huang studied influence of other cations (Na^+ , Mg^{2+} and Ca^{2+}).
- The models proposed by Cuadros and Pytte do not determine a unique set of parameters.
- There are large uncertainties in the determined parameter values in the Cuadros study.
- Pytte et al. and Cuadros et al. did not use the data from the actual studies in order to evaluate the smectite exponent parameter, but fitted it by use of additional data from burial diagenesis, and no independent evaluation was reported.
- A model based on natural analogs like the Pytte study obviously has larger uncertainties regarding boundary conditions and estimation of the independent variables of the model. This especially applies to temperature.

Based on the above facts we consider the Huang et al. model as the best available tool to calculate the extent of montmorillonite to illite transformation also in a KBS-3 type repository.

The present calculations made by use of the Huang model and constants, and by use of realistic potassium concentrations show insignificant transformation of the montmorillonite during the lifetime of the repository. The calculated extent of montmorillonite that will be transformed is less than 1%, which should be compared with the calculated maximum acceptable illitization of

30% based on the design criterion of at least 1 MPa in swelling pressure. The margins to significant transformation is large both with respect to temperature and potassium concentrations.

However, reservations have to be made for the following conditions, which are not covered by the rate model, and which are, or may be, different in the KBS-3 repository compared to the experimental conditions at which the model is based:

- Increased pH conditions (pH 11).
- The liquid to solid ratio (0.25).
- Diffusive silica transport (temperature gradient, high interaction with groundwater).
- Divergent bentonite composition compared to the examined.

Further, the correctness in the model extrapolation from high temperature laboratory conditions to the significantly lower temperature in the repository is not self-evident, since the exact transformation reaction is not clear. However, if the kinetics of quartz crystallization is the rate limiting sub-process then the transformation will be overestimated by the extrapolation.

Other processes than illitization may take place, but these processes are in general even less extensive than the illitization according to the literature. However, the following exceptions have been discussed:

- The thermal gradient over the buffer will induce a concentration gradient i.a. with respect to silica, which can lead to a layer charge increase in the montmorillonite in the inner parts of the buffer and a corresponding silica precipitation in the outer part. Scooping calculations in this work show that both effects are insignificant for near neutral pH conditions, but may lead to noticeable effects at pH 11, which is the upper pH limit in the KBS-3 design criteria.
- The influence of corroding metallic iron on the montmorillonite is not clear. A possible reduction of ferric iron in the octahedral layer will lead to a layer charge increase, which alone do not threaten the sealing properties. However, a general break down of the montmorillonite structure has been observed in recent laboratory experiments.
- A release of silica from the montmorillonite, and a subsequent increase in the layer charge, may take place also without the presence of potassium by precipitation of other silica minerals. The rate of such a process is expected to be slower than illitization, and is not expected to lead to reduced sealing properties without a subsequent potassium uptake, but the role of the total cation concentration is not clear.
- Small cations may at high temperature penetrate into the montmorillonite octahedral layer and thereby neutralize the layer charge in this position. The kinetics of this reaction is not determined and it is unclear if the reaction can take place at repository temperatures.
- The concentration gradient between the groundwater, governed by quartz, and the montmorillonite may lead to significant release of silica if the groundwater turnover is high and pH is increased.

The general conclusion in this study is that the montmorillonite will not transform substantially in a KBS-3 repository. This conclusion is based on natural analogs and to a large extent on the Huang et al. experimental work, which is in a class by itself with respect to quality. A recommendation is therefore that this experimental work should be repeated in a modified way in order to ensure that the expression and the constants are representative also for the specific conditions in a KBS-3 repository. Other obvious suggestions are:

- A similar study to that of Huang et al. in order to determine the kinetics of the reaction with small ion penetration into the octahedral layers in the montmorillonite.
- Determination of diffusive transport properties of silica species, especially at high pH conditions.
- Finally, geochemical transport modeling of possible silica release into groundwater at elevated pH conditions.

References

- Aagard P, Helgeson H C, 1983.** Activity/Composition relations among silicates and aqueous solutions: II. Chemical and thermodynamic consequences of ideal mixing of atoms on homologous sites in montmorillonites, illites and mixed-layer clays, *Clays and Clay Minerals* 31, 207–217.
- Abercrombie H J, Hutcheon I E, Bloch JD and de Caritat P, 1994.** Silica activity and the smectite-to-illite reaction. *Geology*, v. 22, p. 539–542.
- Altaner S P, Ylagan R F, 1997.** Comparison of structural models of mixed-layer illite/smectite and reaction mechanisms of smectite illitization, *Clays and Clay Minerals* 45, 517–533.
- Bauer A, Berger G, 1998.** Kaolinite and smectite dissolution rate in high molar KOH solutions at 35°C and 80°C. *Applied Geochemistry* 13, 905–916.
- Bauer A, Lanson B, Ferrage E, Emerlich K, Velde B, Fanghänel T, 2005.** The fate of smectite before becoming illite in bentonite experiments. International meeting, March 14–18, 2005, Tours, France. *Clays in natural & engineered barriers for nuclear waste confinement*.
- Bethke C M, Altaner S P, 1986.** Layer-by-layer mechanism of smectite illitization and application to new rate law. *Clays and Clay Minerals* 34, 146–154.
- Boles J R, Franks S G, 1979.** Clay diagenesis in the Wilcox Sandstones of southwest Texas. *J. sed. Petrol.* 49, 55–70.
- Burst J F, 1959.** Post diagenetic clay mineral-environmental relationships in the Gulf Coast Eocene in clays and clay minerals. *Clays and Clay Minerals* 6, 327–341.
- Couture R A, 1985.** Steam rapidly reduces the swelling capacity of bentonite. *Nature*, 318, 50–52.
- Cuadros J, Linares J, 1996.** Experimental kinetic study of the smectite-to-illite transformation. *Gehochimica et Cosmochimica Acta.* 60, 439–453.
- Eberl D D, 1978.** The reaction of montmorillonite to mixed-layer clay: The effect of interlayer alkali and alkaline earth cations. *Geochim. Cosmochim. Acta* 42, 1–7.
- Eberl D D, 1980.** Alkali cation selectivity and fixation by clay minerals. *Clays and Clay Minerals* 28, 161–172.
- Eberl D D, Velde B, McCormic T, 1993.** Synthesis of illite-smectite from smectite at earth surface temperatures and high pH. *Clay Minerals* 28, 49–60.
- ECOCLAY II final report, 2005.** Effects of cement on clay barrier performance – phase II. European Commission Contract No. FIKW-CT-2000-00028.
- Elliot W C, Matisoff G, 1996.** Evaluation of kinetic models for the smectite to illite transformation, *Clays and Clay Minerals* 44, 77–87.
- Fritz B, 1985.** Multicomponent solid solutions for clay minerals and computer modeling of weathering processes. In *Chemistry of weathering* (J. I. Drever, ed), NATO ASI series, Series C, vol. 149, D. Reidel pub. Co., 19–34.
- Garrels R M, 1984.** Montmorillonite/illite stability diagrams. *Clays and Clay minerals* 32, 161–166.

- Gaudette H E, Eades J L, Grim R E, 1966.** The nature of illite. *Clays and Clay Minerals* 13, 33–48.
- Greene-Kelly R, 1953.** Irreversible dehydration in montmorillonite. *Clay Miner. Bull.* 2, 52–56.
- Grim R E, Bray R H, Bradley W F, 1937.** The mica in argillaceous sediments, *Amer. Minerl.* 22, 813–829.
- Güven N, Huang W L, 1991.** Effect of octahedral Mg²⁺ and Fe³⁺ substitution on hydrothermal illitization reactions. *Clays and Clay Minerals* 39, 387–399.
- Helgeson H C, Brown T H, Leeper R H, 1969.** *Handbook of Theoretical Activity Diagrams Depicting Chemical Equilibria in Geologic Systems Involving Aqueous Phase at one Atm. and 0° to 300°C.* Freeman, Cooper & Co., San Francisco.
- Hoffmann U, Klemen R, 1950.** Verlust der Austauschfähigkeit von Lithiumionen an Bentonit durch Erhitzung. *Z. Anorg. Chemie* 262, 95–99.
- Horton D G, 1985.** Mixed-layer illite/smectite as a paleotemperature indicator in the Amethyst vein system, Creed, Colorado, USA. *Contrib. Mineral. Petrol.* 91, 171–179.
- Hower J, Mowatt T C, 1966.** The mineralogy of illites and mixed-layer illite/montmorillonites. *Am. Miner.* 51, 825–854.
- Hower J, Eslinger E V, Hower M E, Perry E A, 1976.** Mechanism of burial metamorphism of argillaceous sediments. *Geol. Soc. Amer. Bull.* 87 725–737.
- Hower J, 1981.** Shale diagenesis. In Longstaffe F.J., editor. *Clays and the Resource Geologist.* Mineralogical Association of Canada, Toronto, pp. 60–80.
- Howard J J, Roy D M, 1985.** Development of layer charge and kinetics of experimental smectite alteration. *Clays and Clay Minerals* 33, 81–88.
- Huang W L, Otten G A, 1987.** Smectite illitization: effect of smectite composition. In Program and abstracts, 24th Annual Meeting, The Clay Minerals Society, Socorro, New Mexico 75.
- Huang W L, 1989.** Control on ordering of mixed-layer smectite/illite: an experimental study. In Program and Abstracts, 26th Annual Meeting, The Clay Minerals Society, Sacramento, California, 94.
- Huang W L, Longo J M, Pevear D R, 1993.** An experimentally derived kinetic model for smectite-to-illite conversion and its use as a geothermometer. *Clays and Clay Minerals* 41, 162–177.
- Huertas F J, Caballero E, Jimenes de Cisneros C, Huertas F, Linares J, 2001.** Kinetics of montmorillonite dissolution in granitic solutions. *Applied Geochemistry* 16, 397–407.
- Hökmark H, 1995.** Smectite-to-illite conversion in bentonite buffers; application of a technique for modeling degradation processes. SKB Arbetsrapport AR 95-07, Svensk Kärnbränslehantering AB.
- Hökmark H, Fälth B, 2003.** Thermal dimensioning of the deep repository. Technical Report, TR-03-09, Svensk Kärnbränslehantering AB 2003.
- Inoue A, Kohyama N, Kitagawa R and Watanabe T, 1987.** Chemical and morphological evidence for the conversion of smectite to illite. *Clays and Clay Minerals* 35, 111–120.
- Jennings S, Thompson G R, 1986.** Diagenesis of Plio-Pleistocene sediments of the Colorado River Delta, Southern California. *J. Sed. Petrol.* 56, 89–98.
- Kacandes G H, Barnes H L, Kump L R, 1991.** The smectite to illite reaction: fluid & solids evolution under flow through conditions. In Program and Abstracts, 28th Annual Meeting, The Clay Minerals Society, Houston, Texas, 95.

- Karnland O, Pusch R, Sandén T, 1994.** Effects of cyclic hydration/dehydration on Na and K bentonites. SKB Arbetsrapport AR 94-40, Svensk Kärnbränslehantering AB.
- Karnland O, Sandén T, Johannesson L-E, Eriksen T E, Jansson M, Wold S, Pedersen K, Mutamedi M, Rosborg B, 2000.** Long Term Test of Buffer Material – Final Report on the pilot parcels. SKB TR-00-22, Svensk Kärnbränslehantering AB.
- Karnland O, Olsson S, Nilsson U, Sellin P, 2005b.** Experimentally determined swelling pressures and geochemical interactions of compacted Wyoming bentonite with highly alkaline solutions, Applied Clay Science special issue, Andra Conference in Tours 2005.
- Lantenois S, Lanson B, Muller F, Bauer A, Jullien M, Plancon A, 2005.** Experimental study of smectite interaction with metal Fe at low temperature: 1 Smectite destabilization. *Clays and Clay Minerals*, 53, 597-612.
- Lynch L, Reynolds R C Jr, 1985.** The stoichiometry of the smectite-illite reaction. Program with Abstracts, 21st Annual Mtg, Clay minerals Society, Baton Rouge, La., p. 84.
- Moore D M, Reynolds R C Jr, 1989.** X-Ray Diffraction and the Identification and Analyses of Clay Minerals. Oxford University Press.
- Newman A C D, Brown G, 1987.** The Chemical Constitution of Clays, Mineralogical Society Monograph No.6, ed. A.C.D. Newman, 1987.
- Nilsson A-C, 1995.** Compilation of the groundwater chemistry data from Äspö. Progress Report 25-95-02, SKB, Svensk Kärnbränslehantering AB.
- Niu B, Yoshimura T, Hirai A, 2000.** Smectite diagenesis in Neogene Marine Sandstones and Mudstone of the Niigata Basin, Japan. *Clays and Clay Minerals*, vol. 48 no. 1.
- Ochs M, Talerico C, 2004.** SR-Can. Data and uncertainty assessment. Migration parameters for the bentonite buffer in the KBS-3 concept. SKB, TR-04-18, Svensk Kärnbränslehantering AB.
- Parkhurst D L, Appelo C A J, 1999.** Users guide to PHREEQC (Version 2) – A computer program for speciation, batch reaction, one dimensional transport, and inverse geochemical calculations: U.S. Geological Survey Water-Resources Investigations Report 99-4259, 310 p.
- Powers M C, 1967.** Fluid release mechanisms in compacted marine mudrocks and their importance in oil exploration. *AAPG bull.* 51, 1240–1254.
- Pytte A M, Reynolds R C, 1989.** The thermal transformation of smectite to illite. In *thermal history of Sedimentary Basins*, Editors Naeser N.D. and McCulloh T.H.. Springer-Verlag New York, 133–140.
- Ransom B, Helgeson H C, 1993.** Compositional end members and thermodynamic components of illite and dioctahedral aluminous smectite solid solutions, *Clays and Clay minerals* 41 537–550.
- Roberson H E, Lahann R W, 1981.** Smectite to illite conversion rates: Effects of solution chemistry. *Clays and Clay Minerals* 29, 129–135.
- Sato T, Watanabe T, Otsuka R, 1992.** Effect of layer charge, charge location, and energy change on expansion properties of dioctahedral smectites. *Clays and Clay Minerals*, Vol. 40, No. 1, 103–113, 1992.
- Sato T, Kuroda M, Yokoyama S, Tsutsui M, Pacau C, Ringor C, Fukushi K, Tanaka T, Nakayama S, 2005.** Dissolution kinetics of smectite under alkaline conditions. International meeting, March 14–18, 2005, Tours, France. *Clays in natural & engineered barriers for nuclear waste confinement*.

- Sposito G, Park, S-H, Sutton R, 1999.** Molecular simulations of clay mineral surface geochemistry. Science Highlights in 1998 Annual Report, National Energy Research Computing Center (NERSC), Lawrence Berkeley National Laboratory, p. 61.
- Srodon J, Eberl D D, 1984.** Illite. In Bailey S.W., editor. Micas. Vol. 13 in Reviews in Mineralogy, Mineralogical Society of America, Washington D.C. pp. 495–544.
- Stucki J W, Golden D C, Roth C B, 1984.** The effect of reduction and reoxidation on the surface charge and dissolution of dioctahedral smectites: *Clays and Clay Minerals* 32, 191–197.
- Tardy Y, Fritz B, 1981.** An ideal solid solution model for calculating solubility of clay minerals. *Clays and Clay Minerals* 16, p. 361.
- Velde B, Vasseur G, 1992.** Estimation of the diagenetic smectite illite transformation in time-temperature space. *Amer. Mineral.* 77, 967–976.
- Wei H, Roaldset E, Bjorøy M, 1993.** Kinetics of smectite to illite conversion. EAPG 5th Conference, Stavanger 1993.
- Whitney G, Northrop R, 1988.** Experimental investigation of the smectite to illite reaction: Dual reaction mechanisms and oxygen-isotope systematics. *American Mineralogist*, Vol 73, p. 77–90, 1988.
- Whitney G, 1990.** Role of water in the smectite-to-illite reaction, *Clays and Clay Minerals* 38, 343–350.
- Wilson J, Cressey G, Cressey B, Cuadros J, Vala Ragnarsdottir K, Savage D, Shibata M, 2006.** The effect of iron on montmorillonite stability: (II) Experimental investigation. *Geochimica et Cosmochimica Acta*, 2006, vol 70, p. 323–336.

Appendix 1

Summary of the three reviewed illitization models described in section 2.4.1 and 2.4.2.

| Model | Lab/Field study | Conversion measurement technique | Consistent with principles of chemical kinetics | Parameter control | | [K ⁺] | Arrhenius parameters: | | Rate law | Integrated form |
|-----------|-----------------|----------------------------------|---|------------------------|-------------------------|---|-----------------------|------------------|---|---|
| | | | | Temp | Time | | A ¹⁾ | Ea ²⁾ | | |
| Pytte | Field | XRD | No | Estimated (70–370°C) | Estimated (0–450My) | K-feltspar assumed in equilibrium with Albite | 5.2·10 ⁷ | 33 | $\frac{dS}{dt} = -k \frac{[K^+]}{[Na^+]} S^5$ | $S = \frac{S_0}{\sqrt[4]{1 + 4S_0^4 k \frac{[K^+]}{[Na^+]}} t}$ |
| Huang | Lab | XRD | Yes | Controlled (250–325°C) | Controlled (1–80 days) | Controlled (0.1–6M) | 8.1·10 ⁴ | 28 | $\frac{dS}{dt} = -k [K^+] S^2$ | $S = \frac{S_0}{1 + S_0 k [K^+] t}$ |
| Cuadros 5 | Lab | Silica concentration | No | Controlled (60–200°C) | Controlled (1–180 days) | Controlled (0.025–1M) | 8.5·10 ⁻⁷ | 7.2 | $\frac{dS}{dt} = -k [K^+]^{0.25} S^5$ | $S = \frac{S_0}{\sqrt[4]{1 + 4S_0^4 k [K^+]^{0.25} t}}$ |
| Cuadros 1 | | | | | | | 6.4·10 ⁻⁷ | 7.5 | $\frac{dS}{dt} = -k [K^+]^{0.25} S$ | $S = S_0 e^{-k [K^+]^{0.25} t}$ |

¹⁾ The frequency unit is s⁻¹, the total dimension of A however, depends on the details of each rate law as it is should compensate for the dimension of whatever ion-activity factor is involved.

²⁾ Unit is kcal/mol.